General Disclaimer

One or more of the Following Statements may affect this Document

- This document has been reproduced from the best copy furnished by the organizational source. It is being released in the interest of making available as much information as possible.

- This document may contain data, which exceeds the sheet parameters. It was furnished in this condition by the organizational source and is the best copy available.

- This document may contain tone-on-tone or color graphs, charts and/or pictures, which have been reproduced in black and white.

- This document is paginated as submitted by the original source.

- Portions of this document are not fully legible due to the historical nature of some of the material. However, it is the best reproduction available from the original submission.

EFFECTS OF ROUGHNESS ON THE RADAR RESPONSE TO
SOIL MOISTURE OF BARE GROUND

Remote Sensing Laboratory

RSL Technical Report 264-5

Percy P. Batlivala
Fawwaz T. Ulaby

September, 1975

THE UNIVERSITY OF KANSAS CENTER FOR RESEARCH, INC.

2291 Irving Hill Drive—Campus West   Lawrence, Kansas 66045

THE UNIVERSITY OF KANSAS SPACE TECHNOLOGY CENTER

Raymond Nichols Hall

Center for Research, Inc.

2291 Irving Hill Drive—Campus West   Lawrence, Kansas 66045

Telephone: 913-864-4832

EFFECTS OF ROUGHNESS ON THE RADAR RESPONSE TO
SOIL MOISTURE OF BARE GROUND

Remote Sensing Laboratory
RSL Technical Report 264-5

Percy P. Batlivala
Fawwaz T. Ulaby

September, 1975

REMOTE SENSING LABORATORY

TABLE OF CONTENTS

LIST OF ILLUSTRATIONS

ii

LIST OF ILLUSTRATIONS

Page

LIST OF ILLUSTRATIONS

ABSTRACT

The radar response to soil moisture content was experimentally determined for each of three bare fields with considerably different surface roughnesses at eight frequencies in the 2-8 GHz band for HH and VV polarizations. Analysis of the data indicates that the effect of roughness on the radar backscattering coefficient can be minimized by proper choice of the radar parameters. If, in addition, sensitivity to soil moisture variations and system design constraints are considered, the following radar parameters for an operational soil moisture mapper are recommended: frequency = 4 GHz , angle of incidence range = 7°-15° and either HH or VV polarization. The corresponding sensitivity is about 0.25 dB/.01 g/cm^{3}.

1.0 INTRODUCTION

Soil moisture content is an important parameter in crop yield prediction, runoff prediction and other applications in hydrology, agriculture and meteorology. Remote sensing offers a potential means for the determination of the spatial distribution of moisture content over large areas, within a short time and at a reasonable cost. Among the various electromagnetic sensors, radar is the least affected by atmospheric conditions. It is also time-of-day independent and has the capability of mapping terrain surfaces from satellite altitudes with a spatial resolution compatible with the requirements of the above applications.

The backscattering coefficient, σ^o, of an area extended target, such as a soil medium, is a function of the soil surface roughness and dielectric properties. At microwave frequencies, the dielectric constant of soils is strongly dependent upon the soil moisture content [1,2]. Radar backscatter measurements of bare soil surfaces indicate a high degree of sensitivity to moisture variations, particularly at angles of incidence close to nadir [3,4]. Similar observations have also been noted for vegetation covered fields [5,6], although the presence of the vegetation tends to reduce the sensitivity of σ^o to soil moisture variations. It was further observed that differences in vegetation cover and soil surface roughness affected both, the absolute value of σ^o (for a given moisture content) as well as its sensitivity to moisture variations. For vegetated fields, the correlation coefficient between σ^o and soil moisture content was highest at an angle of incidence of 10° (from nadir) [5].

The present study is a detailed analysis of the effect of roughness on σ^o of bare fields. The objective is to experimentally determine the "optimum" combination(s) of radar parameters (frequency, polarization, angle of incidence range) for mapping soil moisture content. An optimum combination of sensor parameters is defined here such that σ^o of the ground is almost independent of surface roughness while retaining an acceptable sensitivity to soil moisture variations. The present study is limited to bare ground; the combined effects of surface roughness and vegetation cover will be the subject of a future investigation.

2.0 THE EXPERIMENT

Radar backscatter data were acquired from three bare fields having appreciably different surface roughnesses using the University of Kansas truck-mounted 2-8 GHz Microwave Active Spectrometer (MAS) system [7]. The operational characteristics of the radar system are given in Table 1.

A schematic of the test site is shown in Figure 1. For reference purposes, the three fields are designated by S, M and R for smooth, medium rough, and rough, respectively. Photographs of the three fields are shown in Figure 2. By inserting a 4' × 2' × 0.5" metal plate into the soil and photographing it, the surface profiles shown in Figure 3 were obtained. After digitizing each of the profiles at the rate of 10 points per cm (in the horizontal direction), the rms heights were calculated with respect to the mean slope of the ground and found to be 0.88 cm, 2.6 cm, and 4.3 cm for fields S, M and R, respectively. In terms of peak-to-peak variations, typical values for fields S, M and R were 2 cm, 7.5 cm and 15 cm. The combination of rms height and peak-to-peak variation clearly illustrates the wide range of surface roughness represented by the three fields. The surfaces of fields R and M are typical of plowed and plowed-then-disked surface configurations, but the surface of field S is a rather rare case in terms of the majority of terrain surfaces.

After acquiring one radar data set per field with the fields dry, the fields were sprinkler irrigated for 12 hours. Radar data sets were then acquired from the three fields on a rotating basis for a period of 13 days. Each radar data set consisted of measurements of the backscattered return at five angles of incidence ($0°$ (nadir) through $40°$ in $10°$ steps) for HH and VV polarizations (see Table 1) at each of eight frequencies in the 2-8 GHz band. To reduce signal fading, a combination of frequency and spatial averaging was used. Frequency averaging was provided by the 450 MHz bandwidth of the MAS system and spatial averaging was achieved by measuring the return from several different spots on the field. Since the effects of signal fading are most severe at nadir [8], more spatially independent measurements were acquired at nadir than at the higher angles of incidence. The number of measurements at each angle and the calculated 50% and 90% confidence intervals associated with the data at that angle are given in Table 2.

Simultaneous with each radar data set, soil samples were collected at each of the eight sampling locations (Figure 1) of the field under observation. At each

2

Table 1: MAS 2-8 System Specifications

Type: FM-CW
Modulating Waveform: Triangular
Center Frequencies: 2.75, 3.25, 4.75, 5.25, 5.75, 6.25,
                                   6.75, 7.25 GHz

FM Sweep: ΔF 450 MHz
Transmitter Power: 40 mW
IF Frequency: F_{IF} 50 KHz
IF Bandwidth: ΔF_{IF} 6 KHz
Antennas:

    Height above ground: 20 m
    Transmitting antenna diameter: 91.5 cm
    Receiving antenna diameter: 91.5 cm
    Feeds: Log periodic
    Effective Two-way beamwidth: 5.4° at 2.75 GHz / 2.2° at 7.25 GHz

Incidence angle range: 0° (nadir)-80°
Polarization: Horizontal transmit-Horizontal receive (HH)
                                   Vertical transmit-Vertical receive (VV)

Calibration:

    Internal   Delay line
    External   Luneberg lens

3

Table 2: Calculated 50% and 90% confidence limits around the scattering coefficient along with the number of spacially discrete measurements acquired at each angle.

Angle of Incidence	Number of Spacially Discrete Measurements Collected	Confidence Limits* (dB)	
		50%	90%
0	15	+0.6 -0.65	+1.6 -2.0
10	13	+0.65 -0.7	+1.65 -2.05
20	11	+0.7 -1.0	+1.4 -1.6
30	9	+0.5 -0.6	+1.1 -1.2
40	7	+0.5 -0.6	+1.05 -1.2

* Calculated at 5 GHz.
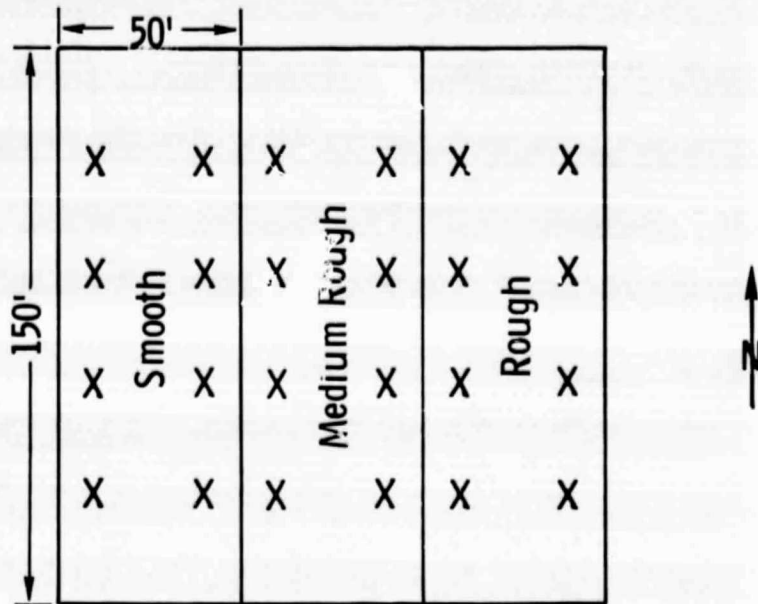
X Indicates Soil Sampling Locations

Figure 1.   Schematic of the test site located at Texas A & M
University agricultural experiment station.

5
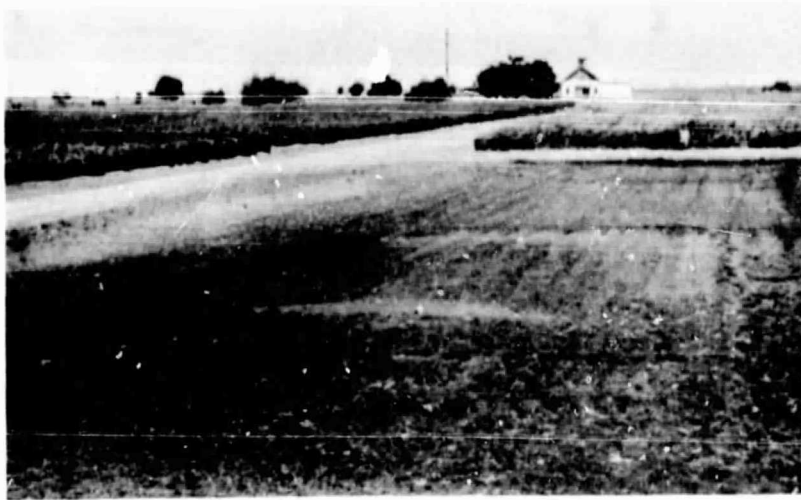
Figure 2. Photographs of bare fields. Soil type is Miller Clay (49% clay, 35% silt, and 16% sand.) (a)Smooth surface, RMS height = 0.88 cm. (b) Medium rough surface, RMS height = 2.6 cm. (c) Rough surface, RMS height = 4.3 cm.

6
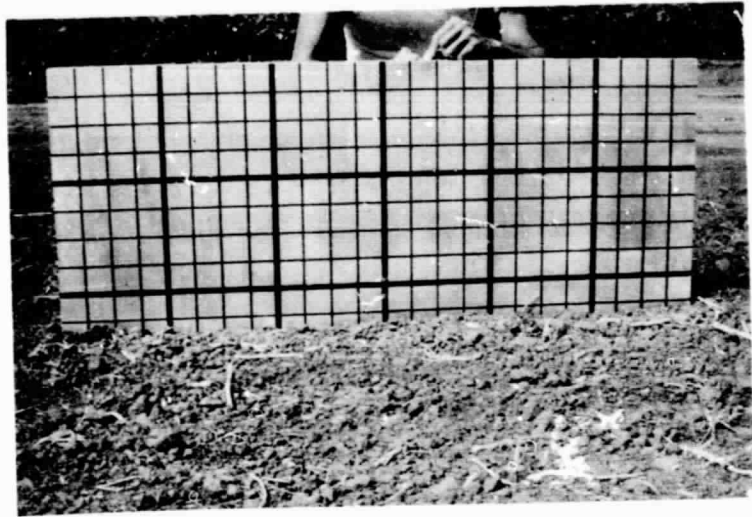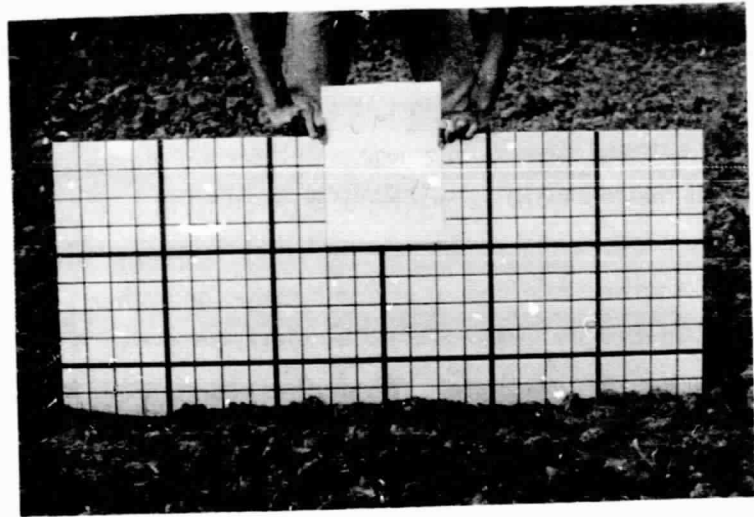
Figure 3. Photographs showing the method used to obtain the surface roughness profile of (a) the smooth field, (b) the medium rough field, and (c) the rough field. The scale on the metal plate is two inches per division.

location samples were collected from five depths: 0-1 cm, 1-2 cm, 2-5 cm, 5-9 cm, and 9-15 cm. These samples were later processed in the laboratory to determine their moisture contents by weight and their bulk densities. Complete listing of the ground-truth and radar data were documented in a separate report [9].

3.0 DEFINITION OF SOIL MOISTURE CONTENT

In the case of a homogeneous soil medium (in terms of its volumetric water content), there is only one obvious quantitative definition of moisture content. The analysis of data to determine the σ° dependence on moisture content is straightforward. Under natural conditions, however, the soil moisture profile with depth is a constant only in the extreme cases of very dry or fully saturated soil. For the in-between cases, the shape of the soil moisture profile of a given field is a complex function of a variety of soil and environmental parameters including texture profile, bulk density profile, temperature profile, rain and irrigation history, and others. Since the dielectric constant of soil is strongly influenced by its moisture content (Figures 4-6), associated with a given moisture profile are two profiles representing the real and imaginary parts of the relative dielectric constant, K_1 and K_2 respectively. At a given microwave frequency, the K_1 and K_2 profiles specify the attenuation profile in the soil medium from which the skin depth can be determined. As an illustration, Figure 7a shows the skin depth as a function of moisture content calculated for a homogeneous medium. It is clear from Figure 7a that at a frequency of 10 GHz, for example, the moisture content in the top 1 cm can be used as an adequate definition of the moisture content responsible for the observed radar return (except for very dry soils).

At a frequency around 1.3 GHz, on the other hand, the backscattered power from a soil medium with a variable moisture profile would most likely include contributions from the air-soil interface as well as from subsurface layers. Thus, in order to analyze the scattering coefficient data in terms of moisture content, surface roughness, soil type, or any other variables of interest, it is necessary to develop a method by which the moisture profile can be represented by an "equivalent" moisture content. The remainder of this section is devoted to a discussion of several approaches for "defining" moisture content.
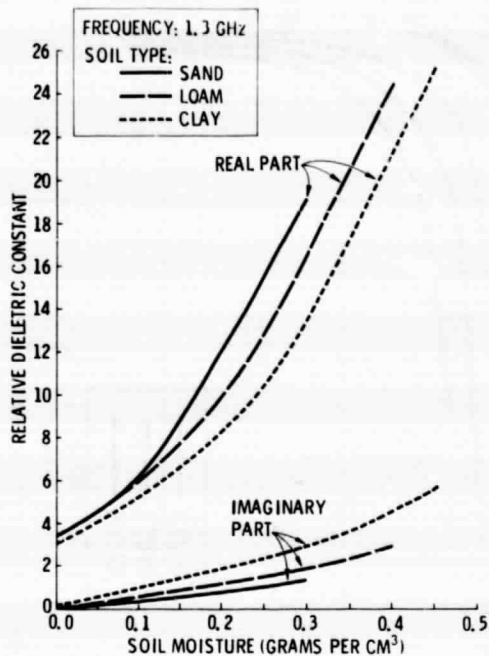
Figure 4. Representative dielectric constant values as a function of volumetric water content for sand, loam, and clay at 1.3 GHz.
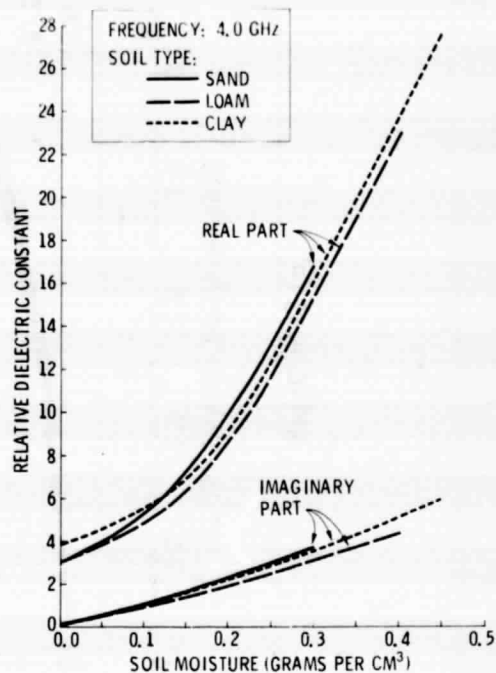
Figure 5. Representative dielectric constant values as a function of volumetric water content for sand, loam, and clay at 4.0 GHz.
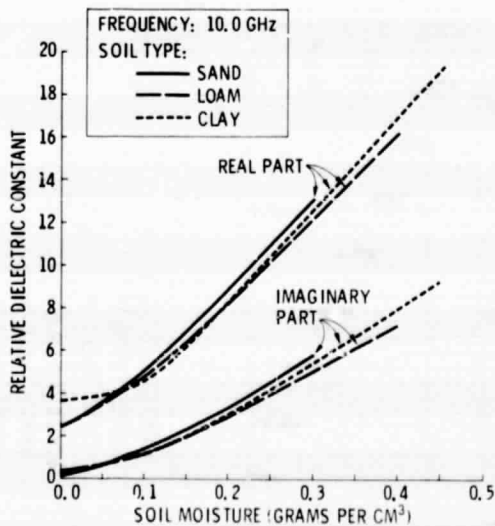
Figure 6. Representative dielectric constant values as a function of volumetric water content for sand, loam, and clay at 10.0 GHz.

9
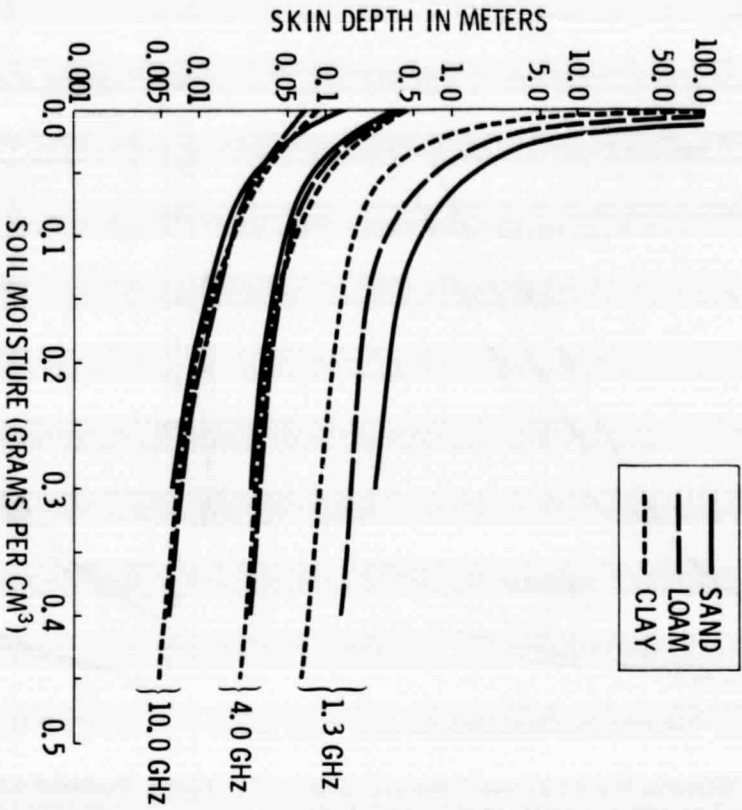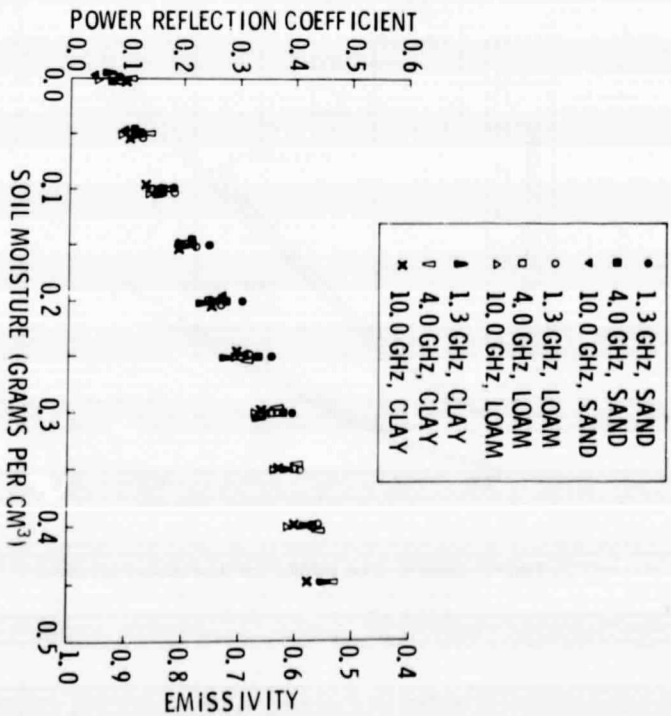
(a) Skin Depth

(b) Power Reflection Coefficient

Figure 7. (a) Skin depth and (b) power reflection coefficient as a function of volumetric water content, frequency and soil type.

10

3.1 Moisture Within Fixed Depths

Soil moisture content in the layer between depths a and b below the surface can be calculated either on a dry weight basis (gravimetric):

$$m_w(a,b) = \frac{1}{(b-a)} \int_a^b \frac{W_w(z) - W_d(z)\, dz}{W_d(z)} \text{, dimensionless} \qquad (1)$$

or on a volumetric basis:

$$m_v(a,b) = \frac{1}{\rho_w(b-a)} \int_a^b \frac{[W_w(z) - W_d(z)]\, \rho_s(z)\, dz}{W_d(z)} \text{, g/cm}^3 \qquad (2)$$

where

z = depth below the surface, cm

a, b = depths of upper and lower ends of the layer, respectively, cm

$W_w(z)$ = profile of the wet weight of the soil, g

$W_d(z)$ = profile of the dry weight of the soil, g

$\rho_s(z)$ = bulk density profile of the soil, g/cm^3

ρ_w = density of water = 1 g/cm^3

Since the surface layer is the most influential in terms of the sensor's response, m_w and m_v are usually evaluated for a = 0. This method has the advantage of simplicity and is probably adequate at frequencies around 10 GHz or higher if b is chosen to be around 1 cm. Between m_w and m_v, the latter is preferred because 1) it incorporates the variation in bulk density with depth and hence is independent of soil compaction and 2) it is physically a better descriptor of the dielectric constant of the soil since it is the total number of water molecules per unit volume of the soil-water mixture that determines the dielectric constant [1]. Hence, all moisture contents discussed in this report are calculated on a volumetric basis.

11

3.2 Moisture Within the Skin Depth

In an attempt to construct the soil moisture profile from multifrequency microwave radiometric measurements, Poe [10] defined the moisture content of the soil in terms of the water within the skin depth. The method was later adapted by Ulaby et al. [4] to the analysis of radar backscatter data from bare soil.

After dividing the soil medium into horizontal layers each having a thickness d, the measured profiles of $W_w(z)$, $W_d(z)$ and $\rho_s(z)$, are used to calculate the volumetric moisture of the ith layer $m_v(i)$, for each i between the surface and the desired depth. The top layer is i = 1. Using the relationships between m_v and K_1 and K_2 (Figure 4-6), $K_1(i)$ and $K_2(i)$ can be determined from which the attenuation coefficient of the ith layer can be calculated:

$$\alpha(i) = \frac{2\pi}{\lambda} \left\{ \frac{K_1(i)}{2} \left[\left(1 + \left(\frac{K_2(i)}{K_1(i)} \right)^2 \right)^{1/2} - 1 \right] \right\}^{1/2} \tag{3}$$

where λ is the wavelength. The skin depth δ is defined by:

$$\int_0^\delta \alpha(z) \ dz = 1 \text{ neper} \tag{4}$$

For the discrete case δ can be determined by summing the attenuation of the layers from the surface downward until the total attenuation is approximately equal to 1 neper. δ is then the product of the number of layers used in the summation by the width d. Using δ as a parameter characterizing the moisture profile of the soil medium under investigation, an equivalent moisture content of a homogeneous medium, m_δ, can be defined such that both media have the same skin depth δ . This equivalent moisture content can be obtained from δ using Figure 7a.

12

Although the skin depth method takes the attenuation of the wave into account, it does not consider the reflection at the air-soil interface and at the interfaces between the various layers.

3.3 Moisture Content Estimated by a Coherent Model

An equivalent moisture content of an inhomogeneous soil medium (with depth) can be defined as the moisture content of a homogeneous soil medium whose power reflection coefficient at the air-soil interface is equal to the power reflection coefficient of the inhomogeneous medium. The power reflection coefficient of a homogeneous medium at nadir is shown in Figure 7b as a function of moisture content, m_v.

The reflection coefficient of a soil medium with varying dielectric constant can be calculated from the solution of Maxwell's equations in a plane-stratified dielectric medium. Casey [11] formulated the solution to this problem in terms of Hill's functions which can be evaluated numerically for a given dielectric profile. Since the method treats the case of a coherent signal incident upon a dielectric medium, it is referred to herein as the Coherent Model, as distinguished from the Incoherent Model discussed in the next section.

The Coherent Model incorporates both attenuation and phase shift in the soil medium which causes the calculated reflection coefficient to be very sensitive to the derivative of the dielectric constant with depth. Hence, unless the soil moisture variation with depth is small over an interval of one wavelength, correct evaluation of the reflection coefficient necessitates accurate knowledge of the moisture profile at depth intervals of the order of $0.1 \lambda_m$ where λ_m is the wavelength in the medium. As an example, at a frequency of 2 GHz, λ_m in a medium with a relative dielectric constant $K_1 = 25$ is 3 cm. From a practical standpoint, collecting soil samples smaller than 1 cm in depth is difficult and time consuming.

3.4 Moisture Content Estimated by an Incoherent Model

Although the wave transmitted by the radar is approximately coherent in nature, the wave backscattered by a target composed of a large number of random scatterers, such as a soil medium, is usually described statistically in a manner similar to the statistics of random noise [12]. This is a result of spatial or frequency averaging (or both). This noise-like (incoherent) description of the backscattered power suggests

13

that the moisture content representation of a soil medium should be based on the power reflection coefficient calculated for an incoherent signal. For a plane surface, the incoherent power reflection coefficient R can be readily calculated from the emissivity of the medium ϵ as follows:

$$R = 1 - \epsilon \tag{5}$$

If the medium is homogeneous, the coherent and incoherent power reflection coefficients are the same. Burke and Paris [13] constructed a numerical procedure for calculating the brightness temperature of a layered medium in terms of the physical temperature and dielectric constant profiles of the soil medium. If the physical temperature profile is assumed constant, their model reduces to an evaluation of ϵ.

The following formulation is adapted from Burke and Paris [13]. With the soil medium divided into n homogeneous layers, the emissivity ϵ at nadir is given by:

$$\epsilon = (1 - R_o) \left[\Gamma_1 P_1 + \sum_{i=2}^{n-1} \left(\Gamma_i P_i \prod_{j=1}^{i-1} Q_j \right) + \prod_{j=1}^{n-1} Q_j \right] \tag{6}$$

where

R_o = power reflection coefficient at air-soil interface

i = layer index (i=1 is surface layer and i=n is a semi-infinite homogeneous layer)

$\Gamma_i = 1 - 1/L_i$

$P_i = 1 + R_i/L_i$

$Q_i = (1-R_i)/L_i$

$L_i = \exp(\alpha_i d_i)$

R_i = power reflection coefficient at the interface between the i and i+1 layers.

α_i = attenuation coefficient of layer i, nepers/cm

d_i = width of ith layer, cm.

From a physical standpoint, the Incoherent Model is limited to cases where the emission is primarily a consequence of absorption in which case volume scattering can be neglected. This condition is satisfied provided the moisture content in the soil is not very small.

3.5 Comparison of Various Soil Moisture Estimates

Figure 8 compares five soil moisture estimates at three frequencies for the 14 profiles obtained from the medium rough field. The five moisture estimates are:

m_1 = moisture content in top 1 cm

m_2 = moisture content in top 2 cm

m_δ = skin depth equivalent moisture content

m_c = Coherent Model equivalent moisture content

m_i = Incoherent Model equivalent moisture content

The profiles as a function of depth are shown in Figure 9. At the lowest frequency (2.75 GHz), for profiles 2, 3, and 7, whose top layers are very moist, all five estimates are quite similar. For the driest condition (profile 1) except for the effective moisture in the skin depth, the remaining four estimates are similar. As the profiles start drying out at the surface the estimates start differing quite appreciably. These patterns are similar at 5.25 GHz and 7.25 GHz.

At the lowest frequency for which the skin depth is comparatively large, the skin depth estimator yields the highest estimate. As the frequency is increased the skin depth decreases resulting in a m_δ value somewhere between m_1 and m_2. The Incoherent Model estimates moistures very close to the 0-1 cm estimator. At the lower frequency m_i values are slightly higher than m_1 but as frequency is increased m_i approaches m_1 and at the highest frequency m_i is slightly lower than m_1. The estimates from the Coherent Model are the lowest and predict erroneously zero moisture contents for a few profiles at 5.25 GHz and 7.25 GHz. There are also large variations in the soil moisture estimates. These variations are caused by the coherent nature of the model as was discussed earlier in section 3.3.

Figure 10 shows soil moisture estimates as a function of frequency for profiles 1, 9 and 2 which were considered dry, moist and very moist. For profiles 1 and 2 the five estimates are quite similar while for the medium moist condition, the skin depth, Coherent and Incoherent Model give widely different estimates.

15
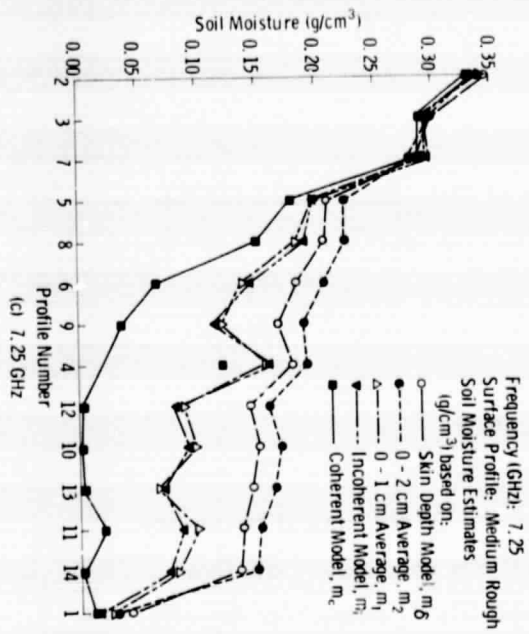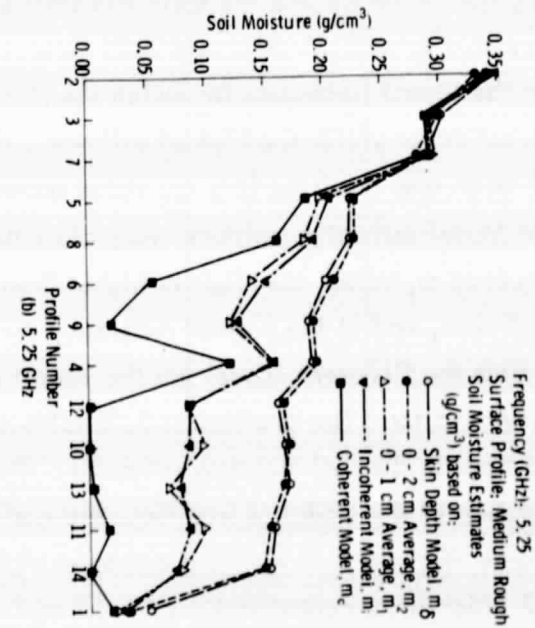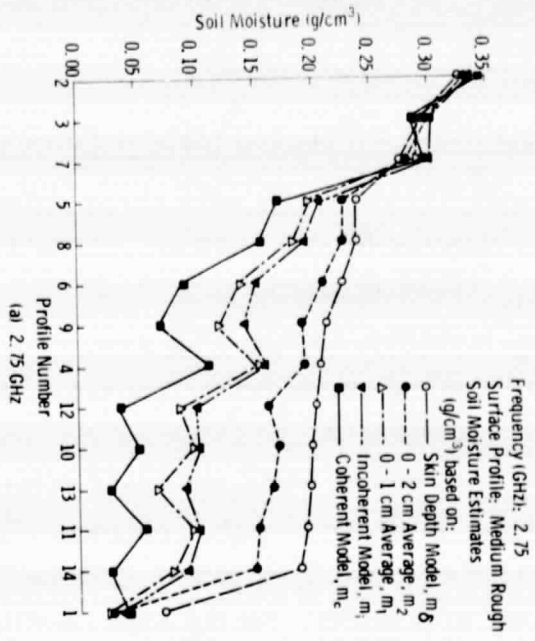
Figure 8. Comparison of five soil moisture estimates for the 14 profiles obtained from the medium rough field for (a) 2.75 GHz, (b) 5.25 GHz, and (c) 7.25 GHz.
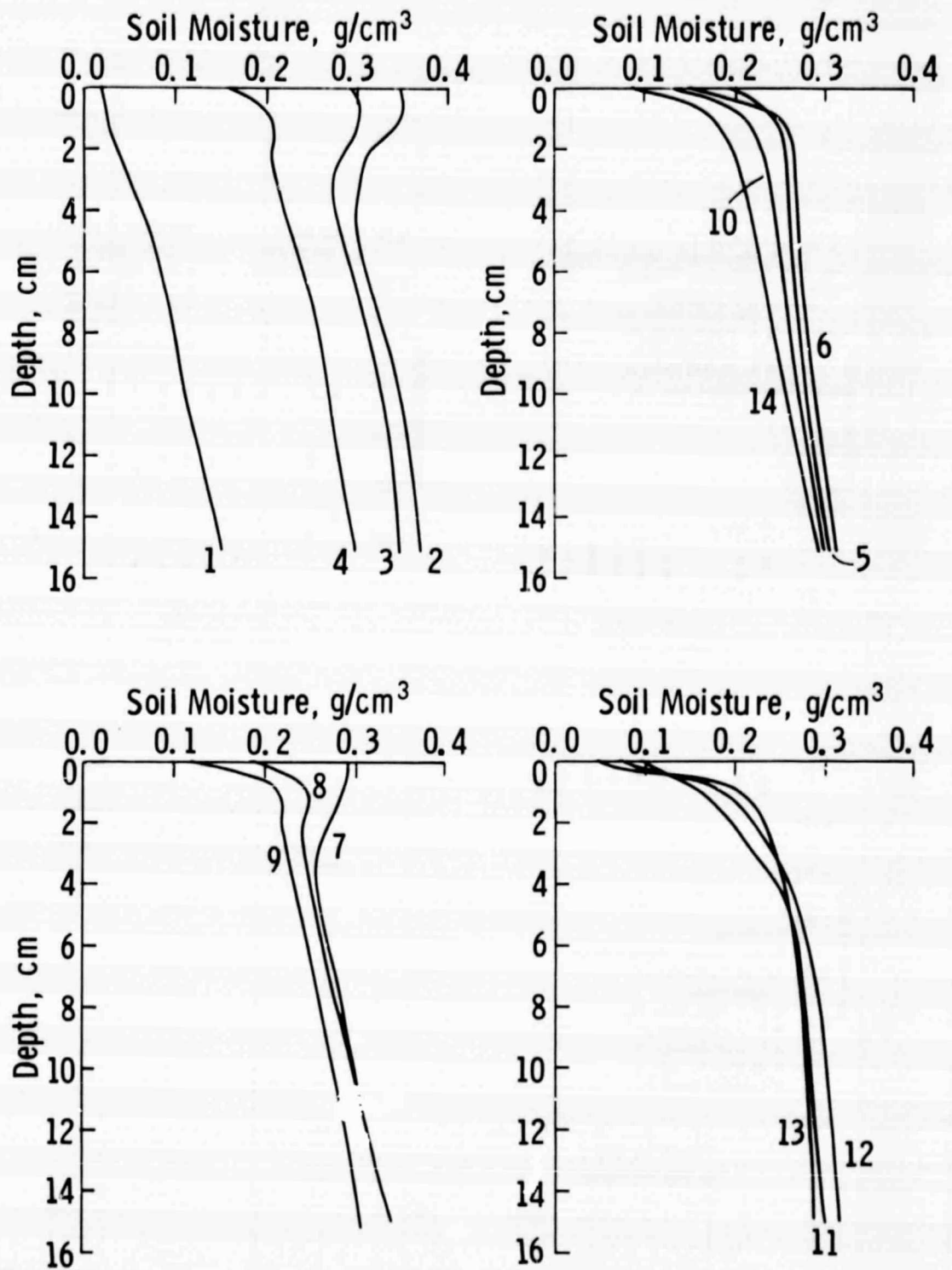
16

Figure 9. Soil moisture profiles for medium rough field. The profile number is indicated next to each profile.
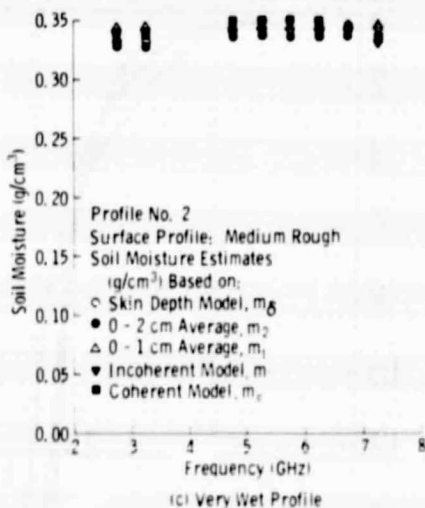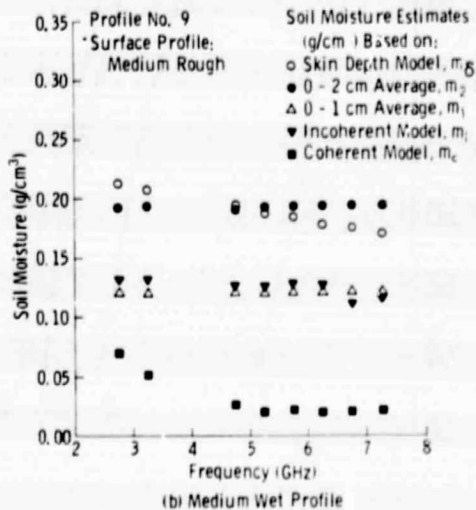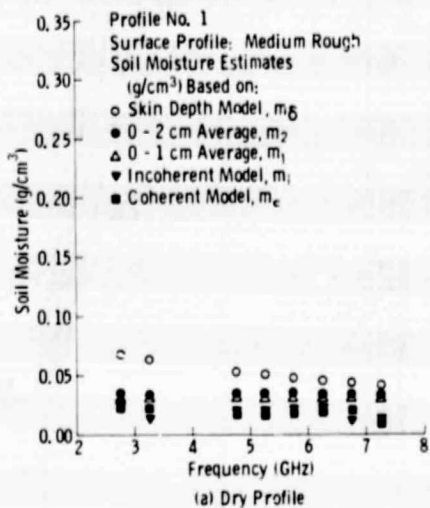
Figure 10. Comparison of five soil moisture estimates as a function of frequency for (a) dry (Profile 1), (b) medium wet (Profile 9), and (c) very wet (Profile 2) cases.

Based on the above comparison of the various methods for representing a given moisture profile with a single moisture content value and based on the physical principles underlying each method, the Incoherent Model estimate m_i has been chosen as the most appropriate. Hence, in all subsequent discussions, m_i will be used exclusively.

3.6 Spatial Variations of Soil Moisture

As was mentioned earlier in section 2, simultaneous with the radar measurements of a given field, soil samples were collected from each of eight sampling locations (Figure 1). After calculating m_i for each of the eight locations, the mean and standard deviation were obtained. Figure 11a-c show σ^o versus time graphs for the smooth, medium and rough fields for 0°, 10° and 20° incidence angles. Plotted on each figure are also soil moisture intervals (average $\pm$ standard deviation). The spatial variation of the soil moisture is appreciable and is attributed mainly to the sprinkler irrigation used and to sampling uncertainty. The σ^o response generally follows the soil moisture changes. Precipitation, which is shown on the graph, caused the surface roughness to change. For example in Figure 11a, σ^o at nadir is larger for the data set taken on the 16th of July as compared to the 14th of July measurement while the soil moisture is actually lower. This is in consequence to the rain on the 14th which smoothed the field surface causing σ^c to increase.

4.0 RESULTS

As surface roughness plays an important role in the backscattering characteristics of bare surfaces, this section is devoted to discussions of the effect of roughness on the angular, spectral and moisture responses of σ^o.

4.1 Angular Response

Figure 12 shows angular responses for the three bare fields with high levels of moisture content. 2.75 GHz, 5.25 GHz and 7.25 GHz were picked as representative frequencies for the low, mid and high range of the 2-8 GHz band. The soil moisture content varies as a function of frequency for each of the surface roughnesses. This

19
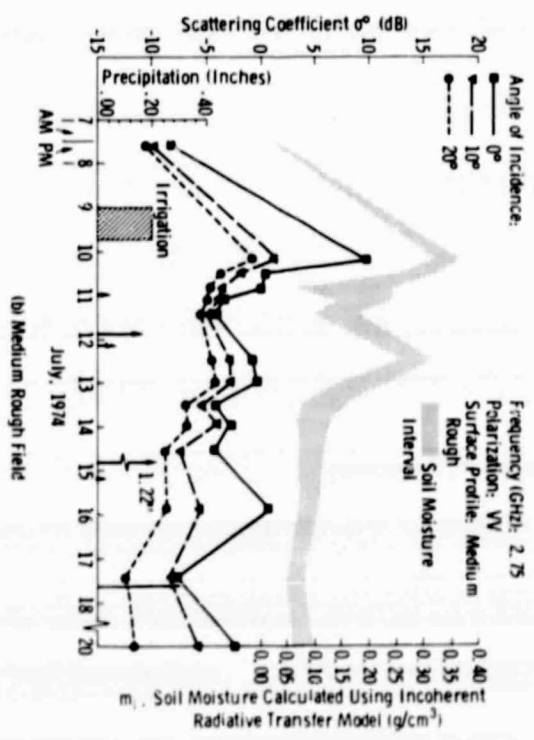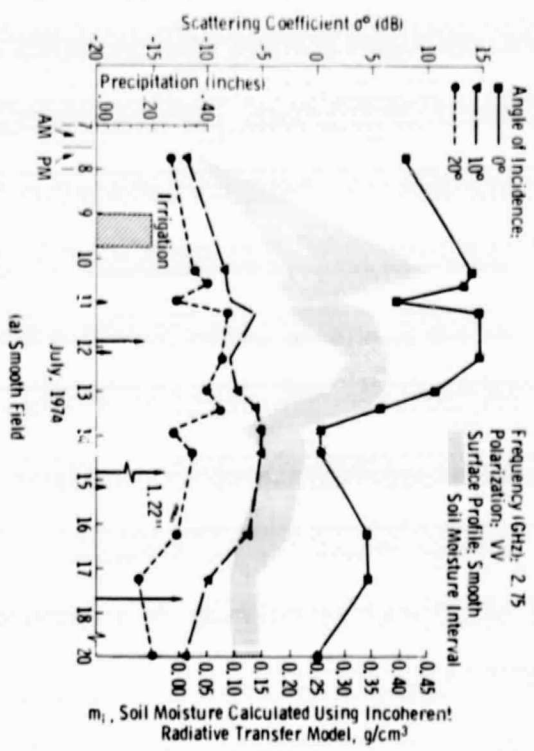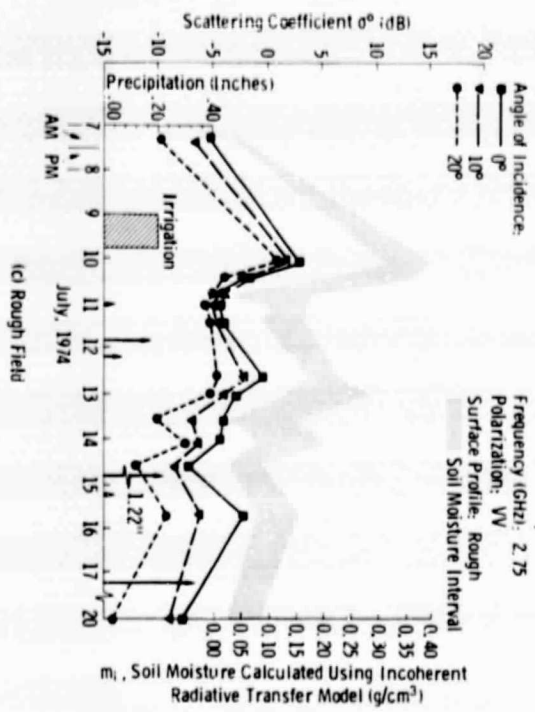
Figure 11. Temporal variations of σ° for (a) the smooth field, (b) the medium rough field, and (c) the rough field. The soil moisture interval is the mean moisture ± standard deviation.
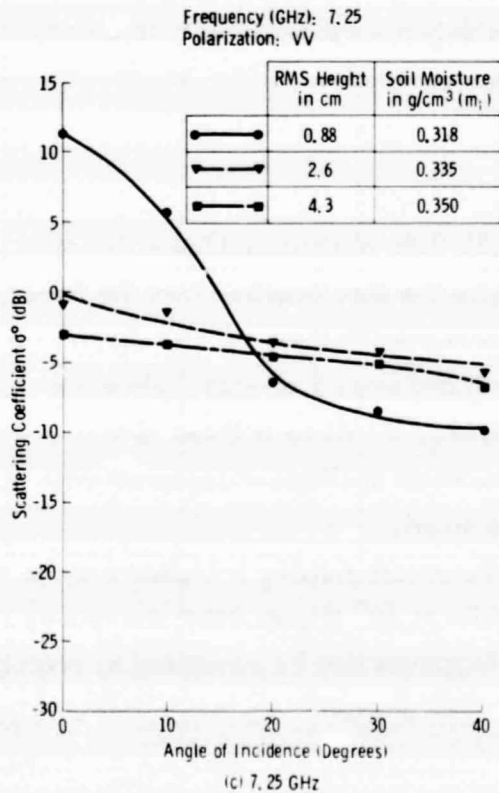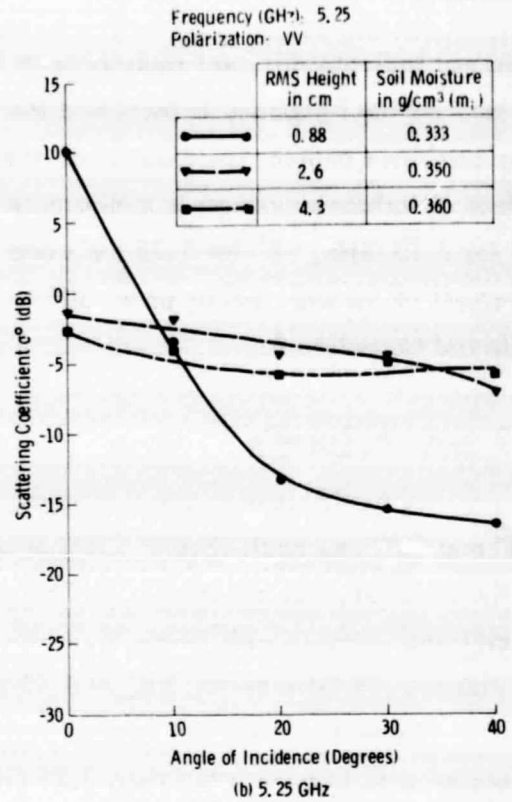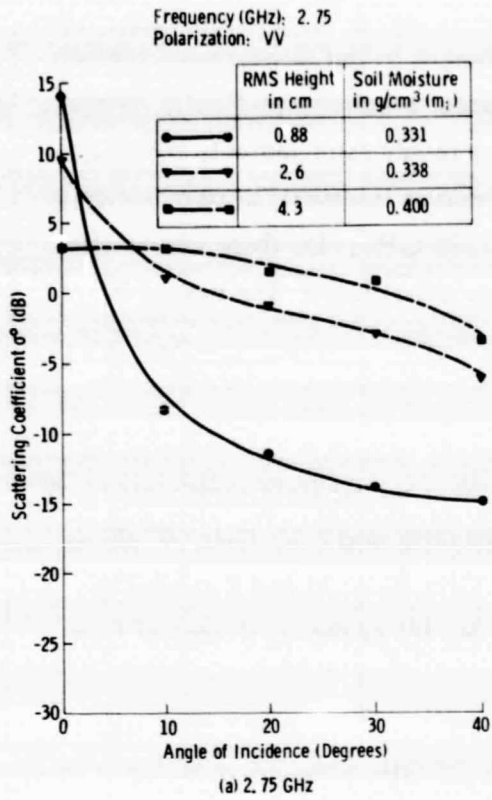
20

Figure 12. Angular response of the scattering coefficient for the smooth, medium rough, and rough fields for high levels of moisture content at (a) 2.75 GHz, (b) 5.25 GHz, and (c) 7.25 GHz.

21

does not indicate different measurements but is inherent in the moisture calculation of m_i. As the frequency is increased the fields appear electromagnetically rougher. The combined angular response for all three surface roughnesses indicate that the effect of surface roughness is minimum (where the curves intersect) at approximately 4° for 2.75 GHz, 10° for 5.25 GHz and 20° for 7.25 GHz. Do these curves also intersect at the same points under different moisture conditions? The answer is deferred to section 5.

4.2 Spectral Response

Figure 13 shows spectral responses for the three wetest field conditions for 0°, 10° and 20°. At nadir (Figure 13a), between 5.25 GHz and 7.25 GHz σ° shows little variation, but between 2.75 GHz and 5.25 GHz fields M and R exhibit a decreasing response with frequency. σ° of field M, for example, decreases from 9.9 dB at 2.75 GHz to -1.5 dB at 5.25 GHz.

Figure 13b shows the spectral responses at 10°. σ° of field R continues to decrease with frequency between 2.75 GHz and 5.25 GHz although at a slower rate, σ° of field M appears almost independent of frequency and field S indicates a strong increasing trend over the entire 2-8 GHz band.

At 20°, unlike fields M and R which show only a weak response to frequency above 5.25 GHz (Figure 13c), σ° of field S increases rapidly.

4.3 Soil Moisture Response

The response of σ° to soil moisture at 2.75 GHz is shown in Figure 14a and 14b for nadir and 10°, respectively. In each figure the data acquired from the three fields is indicated using different symbols. Linear regression lines are also shown along with the calculated correlation coefficient R and slope S of each. Since the slope is an indicator of the response of σ° to moisture, it will be referred to as "sensitivity" S in dB/.01 g/cm^3. The linear correlation coefficient and sensitivity calculated on the basis of all data points are also noted.

At nadir (Figure 14a), the sensitivity of the smooth field S_S is highest and the sensitivity of the rough field S_R is the smallest while at 10° (Figure 14b), the reverse is true. This reversal suggests that the effect of roughness may be minimized by operating at an appropriate angle between 0° and 10°. The dramatic loss in sensitivity of the

Polarization: VV
Angle of Incidence: 0°

	RMS Height in cm	Soil Moisture in g/cm³ (m$_i$)
●——●	0.88	0.333
▼-·-▼	2.6	0.350
■-··-■	4.3	0.360

Polarization: VV
Angle of Incidence: 10°

	RMS Height in cm	Soil Moisture in g/cm³ (m$_i$)
●——●	0.88	0.333
▼-·-▼	2.6	0.350
■-··-■	4.3	0.360

(a) 0° (nadir)

(b) 10° Angle of Incidence

Polarization: VV
Angle of Incidence: 20°

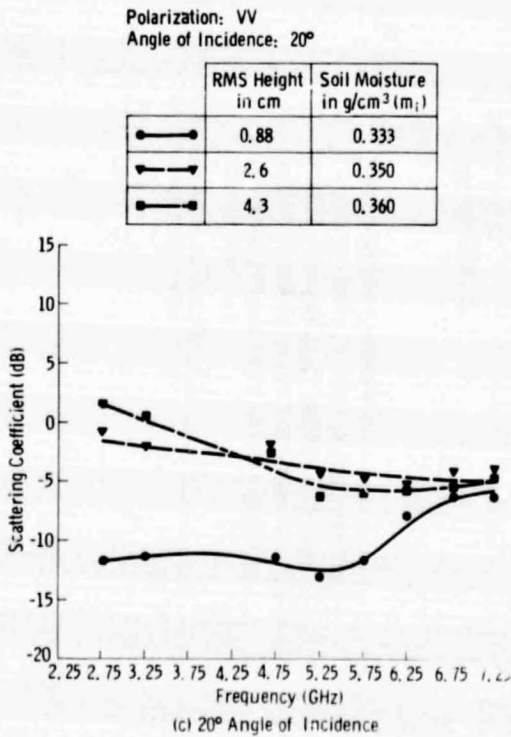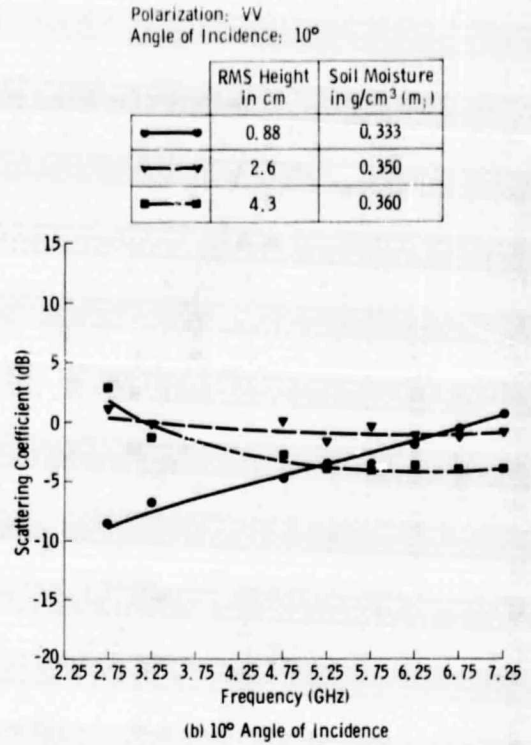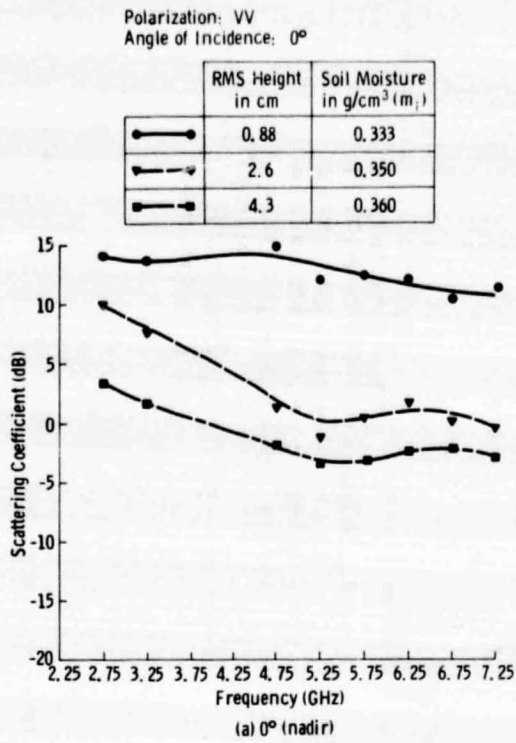|	RMS Height in cm	Soil Moisture in g/cm³ (m$_i$)
●——●	0.88	0.333
▼——▼	2.6	0.350
■——■	4.3	0.360

(c) 20° Angle of Incidence

Figure 13. Spectral response of the scattering coefficient for smooth, medium rough, and rough fields for high level of moisture content at (a) 0° (nadir), (b) 10°, and (c) 20° angle of incidence.
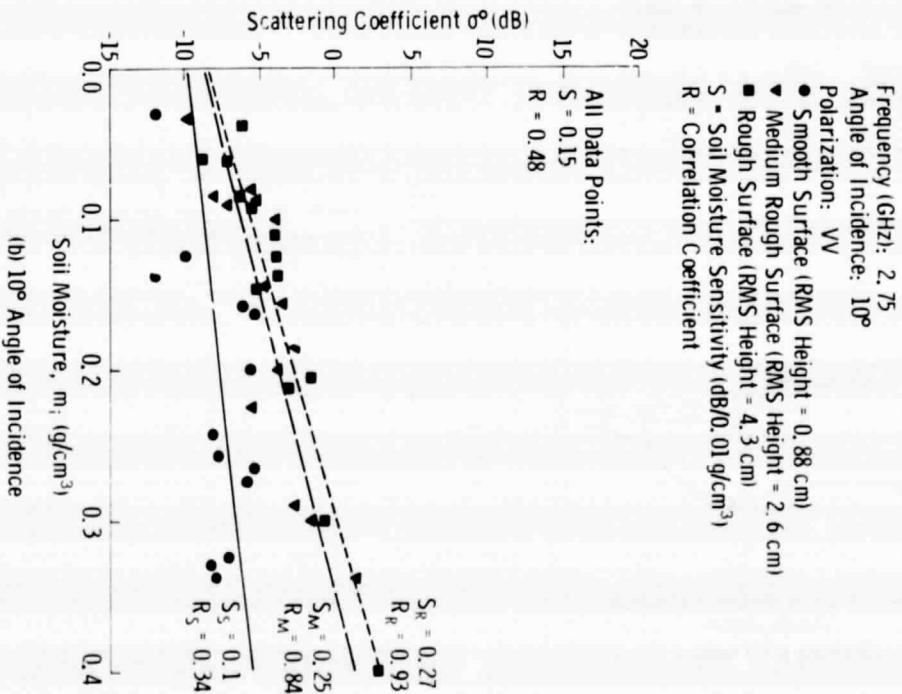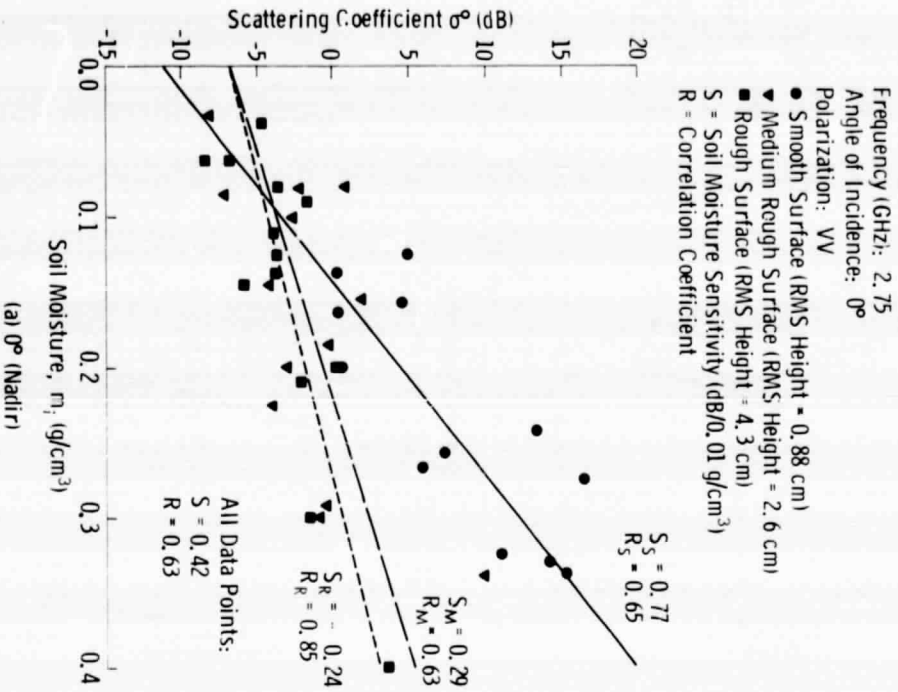
23

Figure 14. Soil moisture responses for the three surface roughness profiles at 2.75 GHz for (a) 0° (nadir) and (b) 10° angle of incidence.

(a) 0° (Nadir)

(b) 10° Angle of Incidence

Frequency (GHz): 2.75
Angle of Incidence: 0°
Polarization: VV
● Smooth Surface (RMS Height = 0.88 cm)
▼ Medium Rough Surface (RMS Height = 2.6 cm)
■ Rough Surface (RMS Height = 4.3 cm)
S = Soil Moisture Sensitivity (dB/0.01 g/cm³)
R = Correlation Coefficient

S_S = 0.77
R_S = 0.65

S_M = 0.29
R_M = 0.63

S_R = - 0.24
R_R = 0.85

All Data Points:
S = 0.42
R = 0.63

Frequency (GHz): 2.75
Angle of Incidence: 10°
Polarization: VV
● Smooth Surface (RMS Height = 0.88 cm)
▼ Medium Rough Surface (RMS Height = 2.6 cm)
■ Rough Surface (RMS Height = 4.3 cm)
S = Soil Moisture Sensitivity (dB/0.01 g/cm³)
R = Correlation Coefficient

S_R = 0.27
R_R = 0.93

S_M = 0.25
R_M = 0.84

S_S = 0.1
R_S = 0.34

All Data Points:
S = 0.15
R = 0.48

24

smooth field as the angle was increased from 0° to 10° is attributed to the smooth appearance of the surface at 2.75 GHz. Since no radar data were acquired between 0° and 10°, an alternative to investigating the moisture response at an angle between 0° and 10° is to investigate the response at 10° but at a higher frequency. Increasing the frequency causes the surfaces to appear rougher which is somewhat comparable to decreasing the angle of incidence. Figure 15 shows the moisture response at 10° and 4.75 GHz. The correlation coefficient calculated for all the data points regardless of surface roughness is 0.75. Considering the uncertainty associated with the measurement of σ° (Table 2) and the uncertainty associated with the measurement of m_i (Figure 11), the response shown in Figure 15 is very encouraging. With a sensitivity of 0.25 dB/.01 g/cm^3, the expected change in return between moisture levels of 0.05 g/cm^3 (relatively dry) and 0.35 g/cm^3 (very wet) is 7.5 dB.

5.0 CHOICE OF OPTIMUM SYSTEM PARAMETERS

In the previous section angular, spectral and soil moisture responses were studied for all three roughnesses as a function of the various system parameters. It was demonstrated that the effects of roughness can be reduced by proper choice of frequency and angle of incidence, while at the same time retaining good sensitivity to soil moisture. In this section a more comprehensive analysis of the dependence of σ° on moisture, surface roughness, frequency, polarization and angle of incidence is presented in a unified quantitative approach.

5.1 Effect of Roughness

The parameter chosen to represent roughness in this study is rms height, h. As the radar responds to both large scale and small scale roughness this representation is undoubtedly not optimal. However as an initial estimator (in terms of ease of measurement) rms height seems to be an adequate quantifier. Linear regression lines of σ° as a function of soil moisture content were calculated for each individual surface roughness (rms heights of 0.88 cm, 2.6 and 4.3 cm) at each angle of incidence, polarization and frequency combination. The σ° values shown in Figures 16-18 were calculated using the regression equations and selected values of soil moisture. Figure 16 shows σ° versus h curves at nadir for 2.75 GHz, 4.75 GHz and 7.25 GHz. As
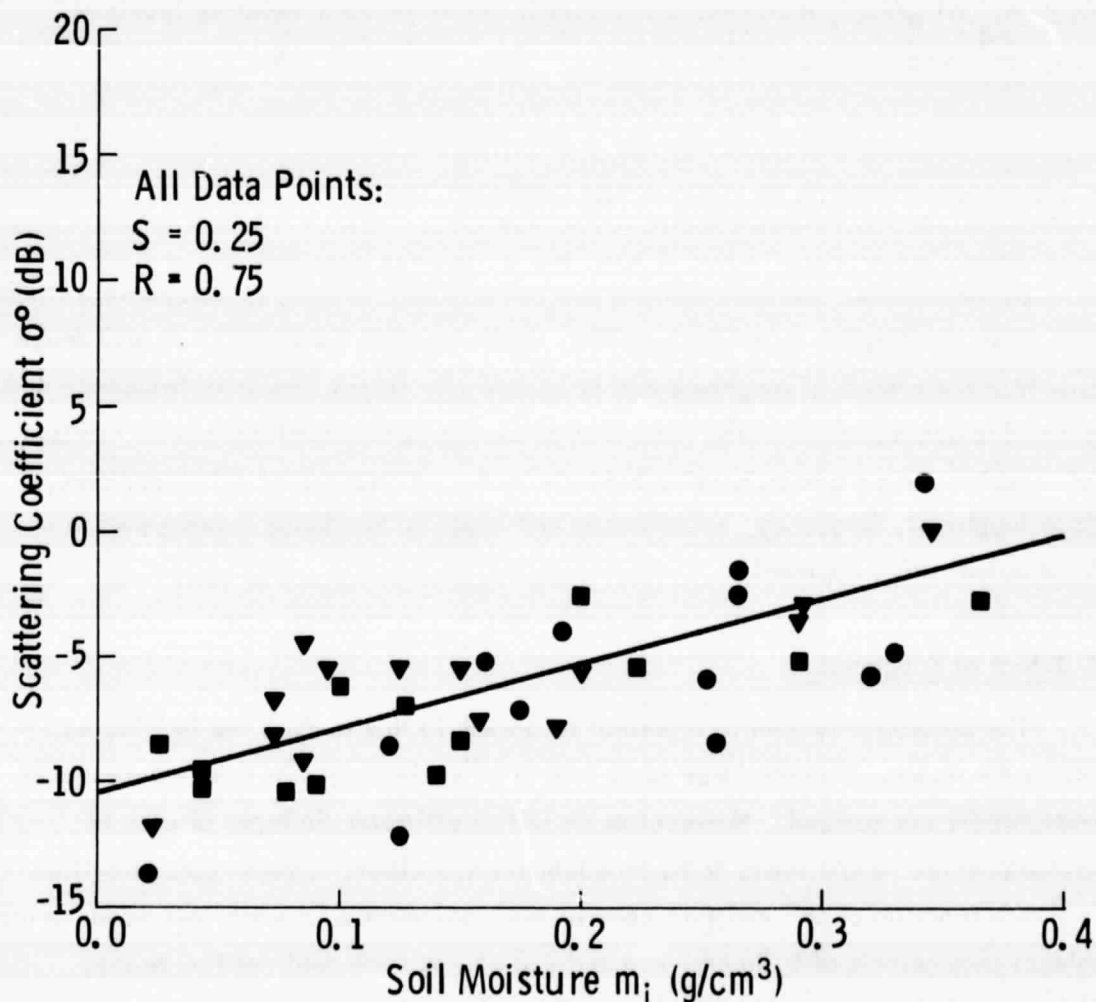
Figure 15. Scattering coefficient response as a function of soil moisture for the combination of all three surface roughness profiles.

Angle of Incidence: 0°
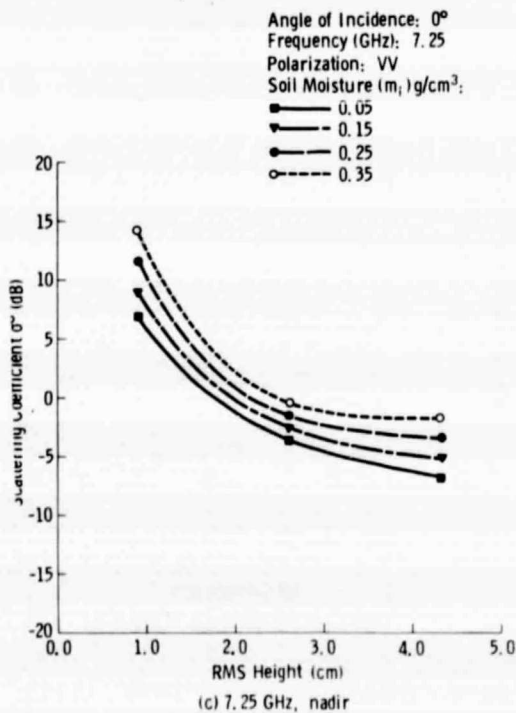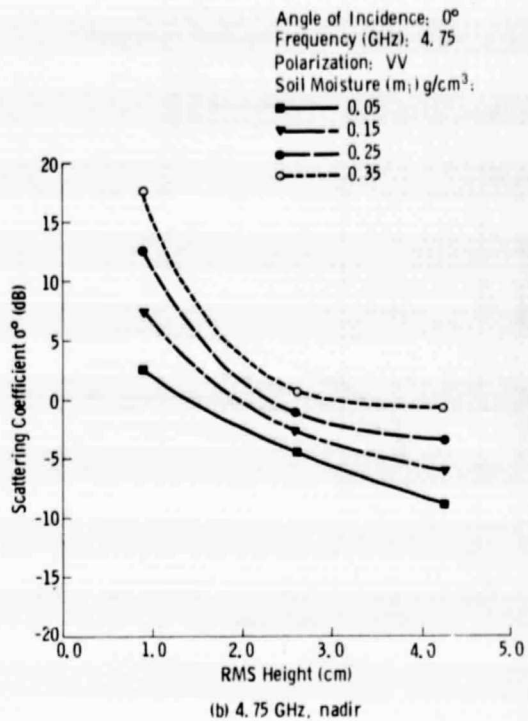Frequency (GHz): 2.75
Polarization: VV
Soil Moisture (m$_i$) g/cm^3:
■——— 0.05
▼—— 0.15
●—·— 0.25
○------ 0.35

(a) 2.75 GHz, nadir

Angle of Incidence: 0°
Frequency (GHz): 4.75
Polarization: VV
Soil Moisture (m$_i$) g/cm^3:
■——— 0.05
▼—— 0.15
●—·— 0.25
○------ 0.35

(b) 4.75 GHz, nadir

Angle of Incidence: 0°
Frequency (GHz): 7.25
Polarization: VV
Soil Moisture (m$_i$) g/cm^3:
■——— 0.05
▼—— 0.15
●—·— 0.25
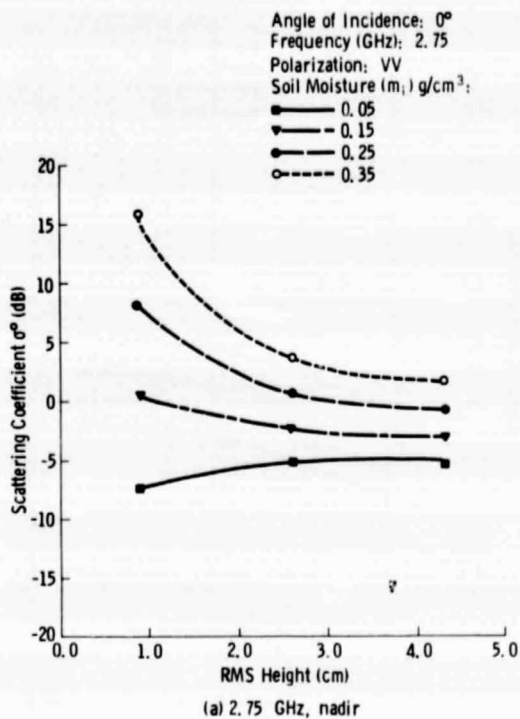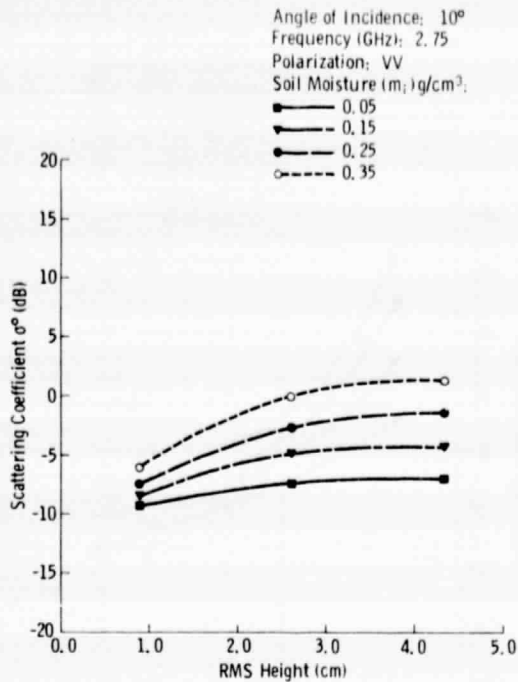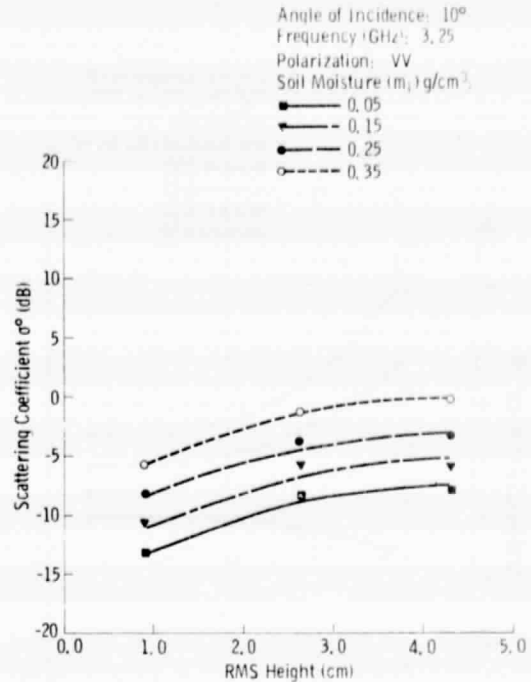○------ 0.35

(c) 7.25 GHz, nadir

Figure 16. Scattering coefficient as a function of surface roughness at nadir for four moisture conditions at (a) 2.75 GHz, (b) 4.75 GHz, and (c) 7.25 GHz.
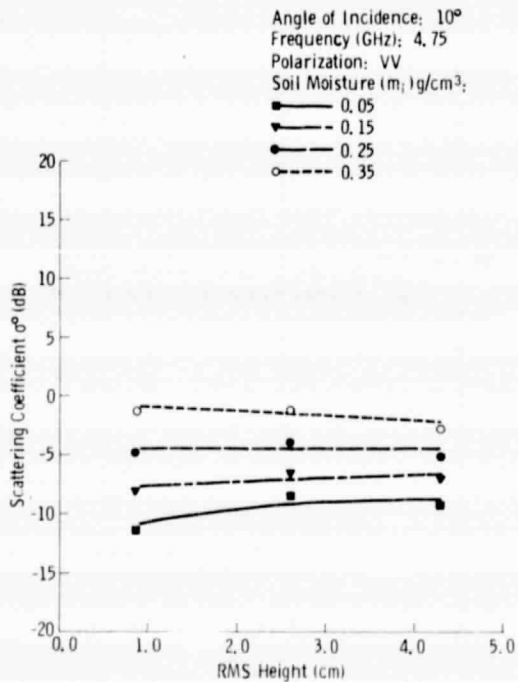
27

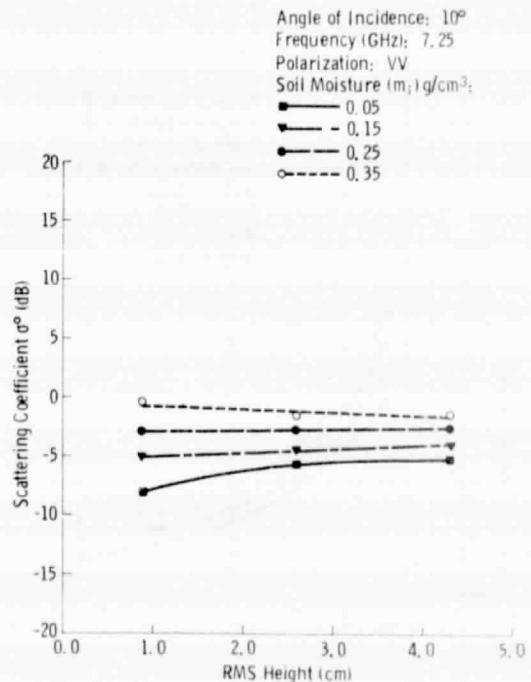Figure 17. Scattering coefficient as a function of surface roughness at an angle of incidence of 10° for four moisture conditions at (a) 2.75 GHz, (b) 3.25 GHz, (c) 4.75 GHz, and (d) 7.25 GHz.
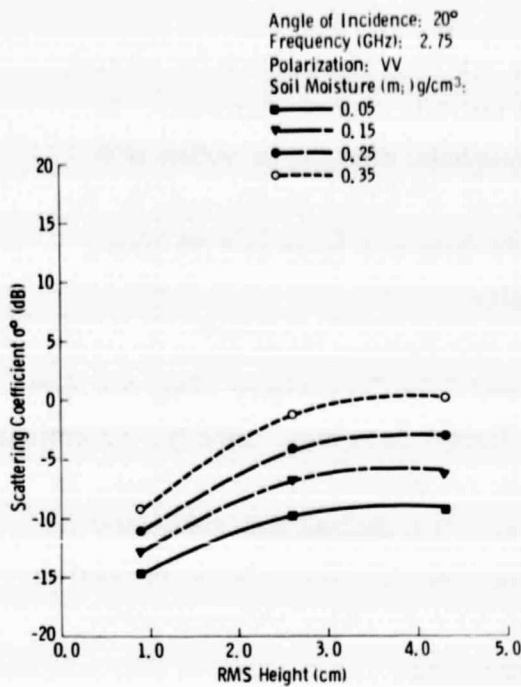
28

(a) 2.75 GHz, 20° Angle of Incidence

(b) 4.75 GHz, 20° Angle of Incidence
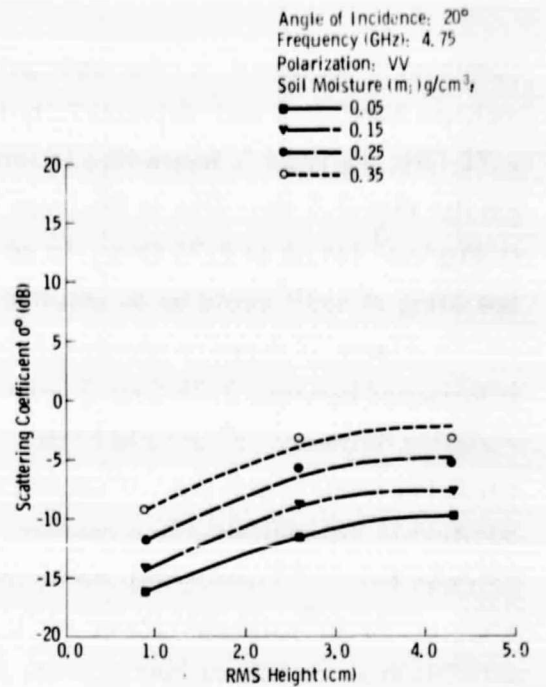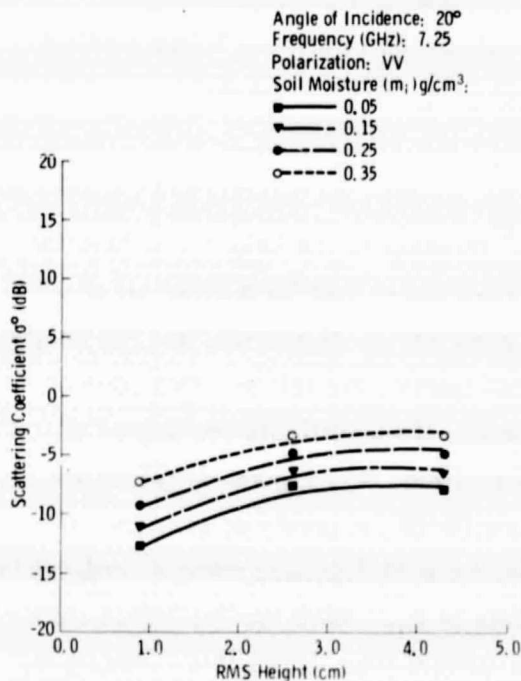
(c) 7.25 GHz, 20° Angle of Incidence

Figure 18. Scattering coefficient as a function of surface roughness at an angle of incidence of 20° for four moisture conditions at (a) 2.75 GHz, (b) 4.75 GHz, and (c) 7.25 GHz.

frequency is increased (a) the radar gets more sensitive to roughness for all soil moisture conditions and (b) sensitivity to soil moisture changes decreases. At 2.75 GHz the radar is insensitive to surface roughness changes for values of h greater than 2.5 cm. Due to the large change of σ^o with h particularly for the $0.35 g/cm^3$ (14 dB at 2.75 GHz, 18 dB at 4.75 GHz and 16 dB at 7.25 GHz), operating at nadir would be an unsuitable choice.

Figure 17 shows roughness responses at four frequencies at 10°. As frequency is increased between 2.75 GHz (Figure 17a) and 7.25 GHz (Figure 17d), the total variation between σ^o of field S and σ^o of field R decreases. Ideally, the optimum condition is one where the σ^o moisture curves are parallel horizontal lines. In addition to independence to roughness, however, it is desired that the separation between the σ^o lines corresponding to different moisture levels be as far apart as possible. At 10°, the data shown in Figure 17c at 4.75 GHz, VV polarization, satisfies these conditions best over the 2-8 GHz band.

At 20° (Figure 18), variations in σ^o due to variations in h also decrease with frequency, but it appears that the condition of almost roughness independence requires a frequency higher than 7.25 GHz. Increasing frequency or angle, however, results in a reduction in the magnitude of the sensitivity S (represented in the figures in terms of the separation between the different curves).

5.2 Constant σ^o Contours

Figures 16-18 have indicated the σ^o response to rms height as a function of angle of incidence and frequency. It is also evident that for a given set of sensor parameters there exists more than one combination of moisture and rms height for which σ^o is the same. For an operational system, the soil moisture content is to be predicted on the basis of σ^o measurements. To investigate the degree of uncertainty associated with the prediction of m_i from σ^o, Figures 19-21 were constructed. Using the curves shown in Figures 16-18, a family of constant σ^o contours were generated with h and m_i as axes for each frequency-angle combination.

For minimum uncertainty in the estimate of m_i, which implies independence of h, the σ^o contours should be as close to vertical lines as possible. Among the frequency-angle combinations shown in Figures 19-21, the data at 10° and 4.75 GHz (Figure 20c) approaches the desired condition the best. Since the data in Figures 19-21 are the same data plotted earlier in Figures 16-18, the conclusion reached in
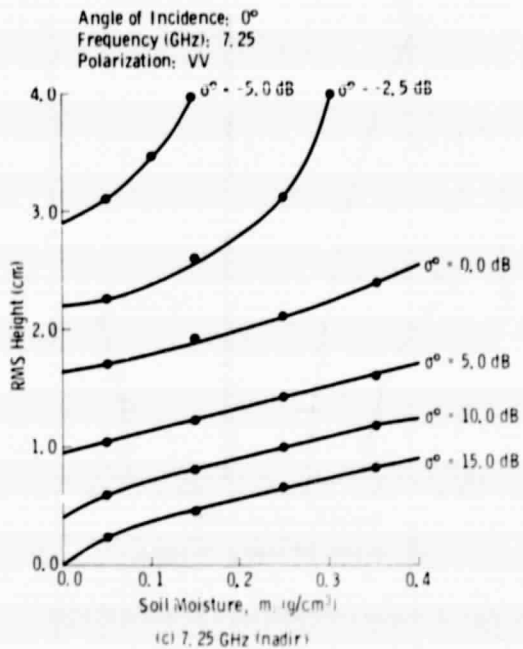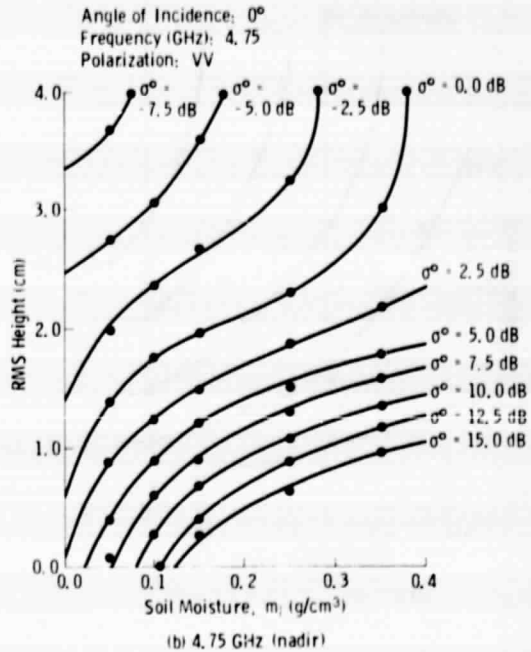
30

Figure 19. RMS height versus soil moisture graphs indicating constant σ° contours at nadir for (a) 2.75 GHz, (b) 4.75 GHz, and (c) 7.25 GHz.
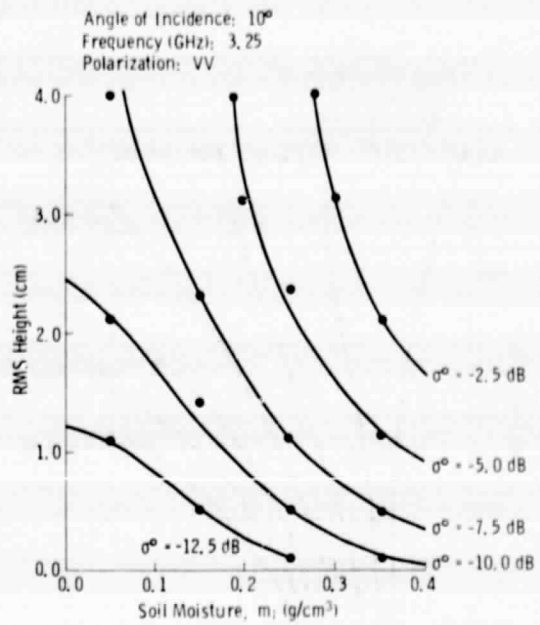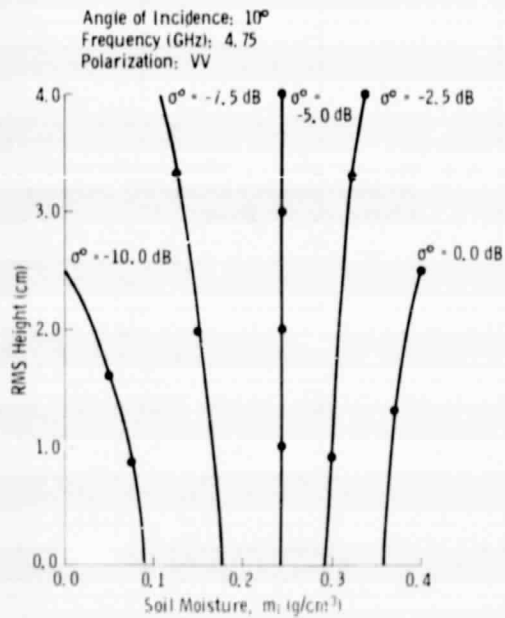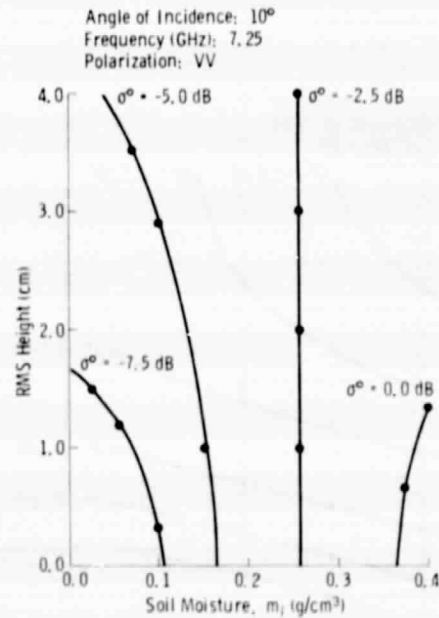
Figure 20. RMS height versus soil moisture graphs indicating constant $\sigma^{-\circ}$ contours at an angle of incidence of 10° for (a) 2.75 GHz, (b) 3.25 GHz, (c) 4.75 GHz, and (d) 7.25 GHz.

(a) 2.75 GHz, 20° Angle of Incidence

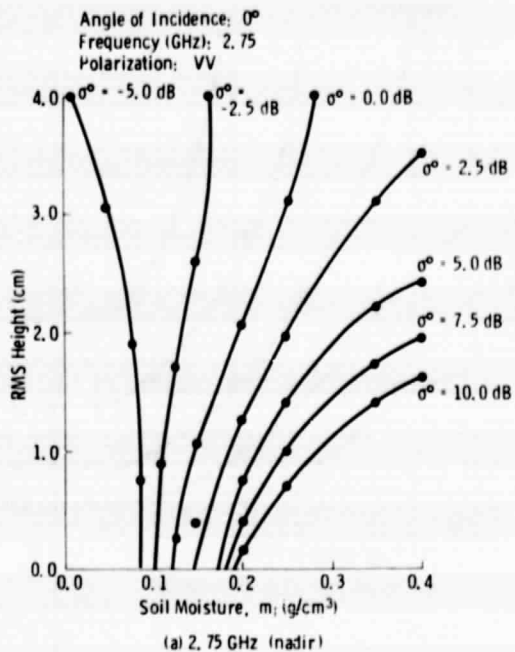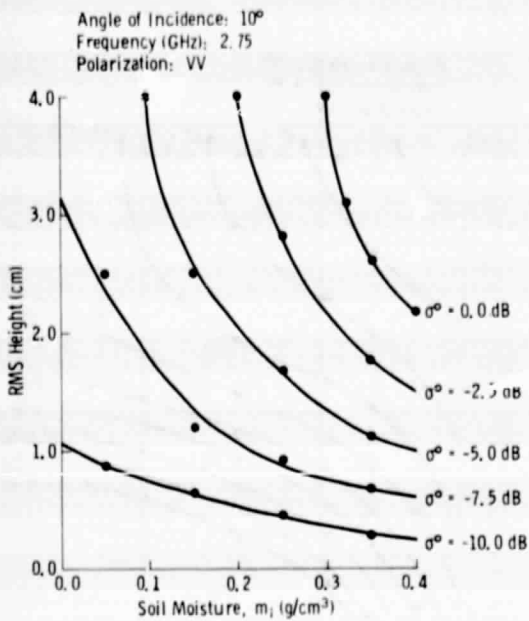(b) 4.75 GHz, 20° Angle of Incidence

(c) 7.25 GHz, 20° Angle of Incidence

Figure 21. RMS height versus soil moisture graphs indicating constant $\sigma^{-\circ}$ contours at an angle of incidence of 20° for (a) 2.75 GHz, (b) 4.75 GHz, and (c) 7.25 GHz.
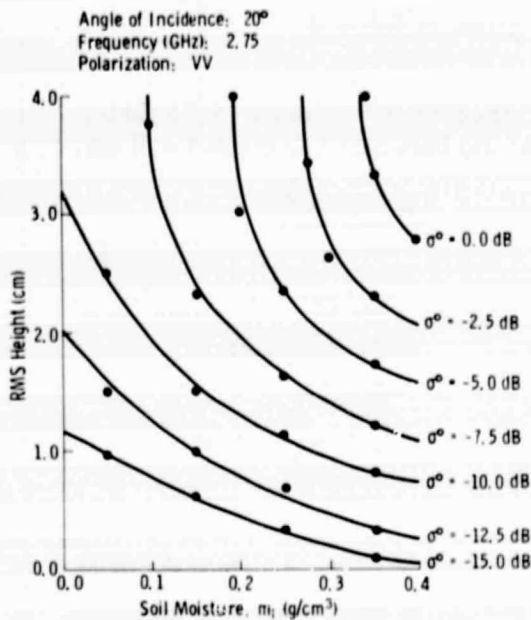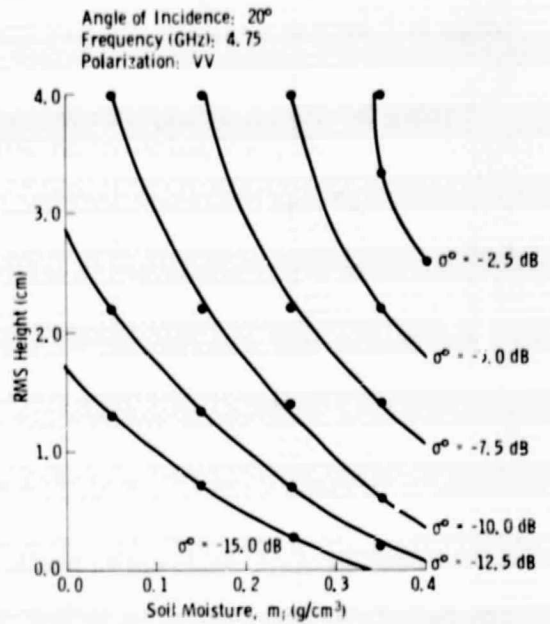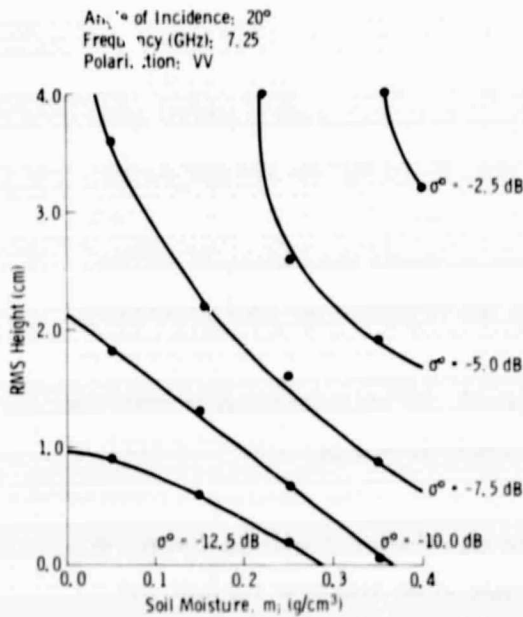
this section is the same as the conclusion reached in the previous section. The σ^o
contour type of presentation is useful in determining the expected uncertainty in
the estimate of m_i over a given range of h. For example, at 4.75 GHz, 10°, and
VV polarization, the m_i ranges associated with the contours of Figure 20c over a
range of h between 1.0 cm and 4.0 cm are as given in Table 3:

Table 3: Moisture ranges corresponding to specific σ^o values at 4.75 GHz,
10°, VV polarization with h varying between 1.0 cm and 4.0 cm.

σ^o (dB)	m_i (g/cm^3)
-10	$\leq .075$
- 7.5	$0.11 \leq m_i \leq 0.17$
- 5.0	0.24
- 2.5	$0.3 \leq m_i \leq 0.34$
0.0	≥ 0.36

The contours depicted in Figures 19-21 suggest that the moisture estimate
can perhaps be improved even further through the use of more than one frequency.
This topic is, however, deferred to a future reporting.

5.3 Regression Analysis

The analyses presented in the previous sections indicate that the angular
region of interest in terms of soil moisture mapping is between 0° (nadir) and
20°. The radar data were acquired at five angles, 0° to 40° in 10° steps. In
order to expand the number of available angles between 0° and 20°, non-linear
interpolation of the angular response was used to evaluate the values of σ^o at
3.3^o, 6.7^o, 13.3^o and 16.7^o. This procedure was repeated for each frequency-
polarization data set. Thus now, the new data base consists of eight frequencies
x nine angles x two polarization = 144 data sets of σ^o as a function of moisture
for each of the three fields. Linear regression analysis was performed for each of
these data sets. After conducting this process for each of the moisture representations
defined in section 3, it was determined that the correlation coefficient was the
highest for the overwhelming majority of the cases when moisture content was
represented by m_i, the Incoherent Model definition. This result confirms its superior
physical basis (in comparison to the other definitions of moisture content) in terms
of the signal-target interaction process.

34

An example is shown in Figure 22 where the calculated correlation coefficient R between σ^o and moisture content is plotted as a function of frequency for moisture content in the 0-1 cm layer, moisture content based on the Skin Depth model and moisture content based on the Incoherent Model. The results clearly indicate that overall, R is highest when m_i is used to represent moisture content.

The results of the regression analyses will be presented for three cases. First, results of the σ^o response to moisture for each individual field will be presented. Second, results of the σ^o response to moisture for fields M and R together will be presented. This case was included to demonstrate the effect of adding field S, which is presented last. Since field S is almost an extreme case in terms of surface roughness of fields under natural conditions, the design of an operational radar for mapping soil moisture should be based on an extrapolation between the results of the last two cases.

For each of the three cases the procedure outlined below was followed: correlation coefficients and sensitivities were calculated for each angle of incidence, polarization and frequency combination. Then for a given angle of incidence and polarization combination the optimum (highest) correlation coefficient was picked. The frequency at which this optimum value occurred was noted along with the corresponding sensitivity. To facilitate brevity the frequency and sensitivity associated with the optimum correlation coefficient are henceforth termed "optimum frequency" and "optimum sensitivity" respectively.

5.3.1 Moisture Response for Individual Roughnesses

Figure 23 presents the "optimum" radar performance of field S as a function of angle of incidence. The optimum performance is defined in terms of three parameters: optimum frequency, optimum correlation coefficient and optimum sensitivity. It should be emphasized that at a given angle and for a given polarization, these three parameters are coupled together and hence, should be interpreted as a group. For example, the optimum correlation coefficients at 10° and 20° (Figure 23a) are approximately the same, and similarly are the optimum frequencies (Figure 23c), but the sensitivity at 10° (Figure 23b) is larger than the sensitivity at 20° by about a factor of 1.5. Hence, better performance would be expected at 10° compared with 20°.
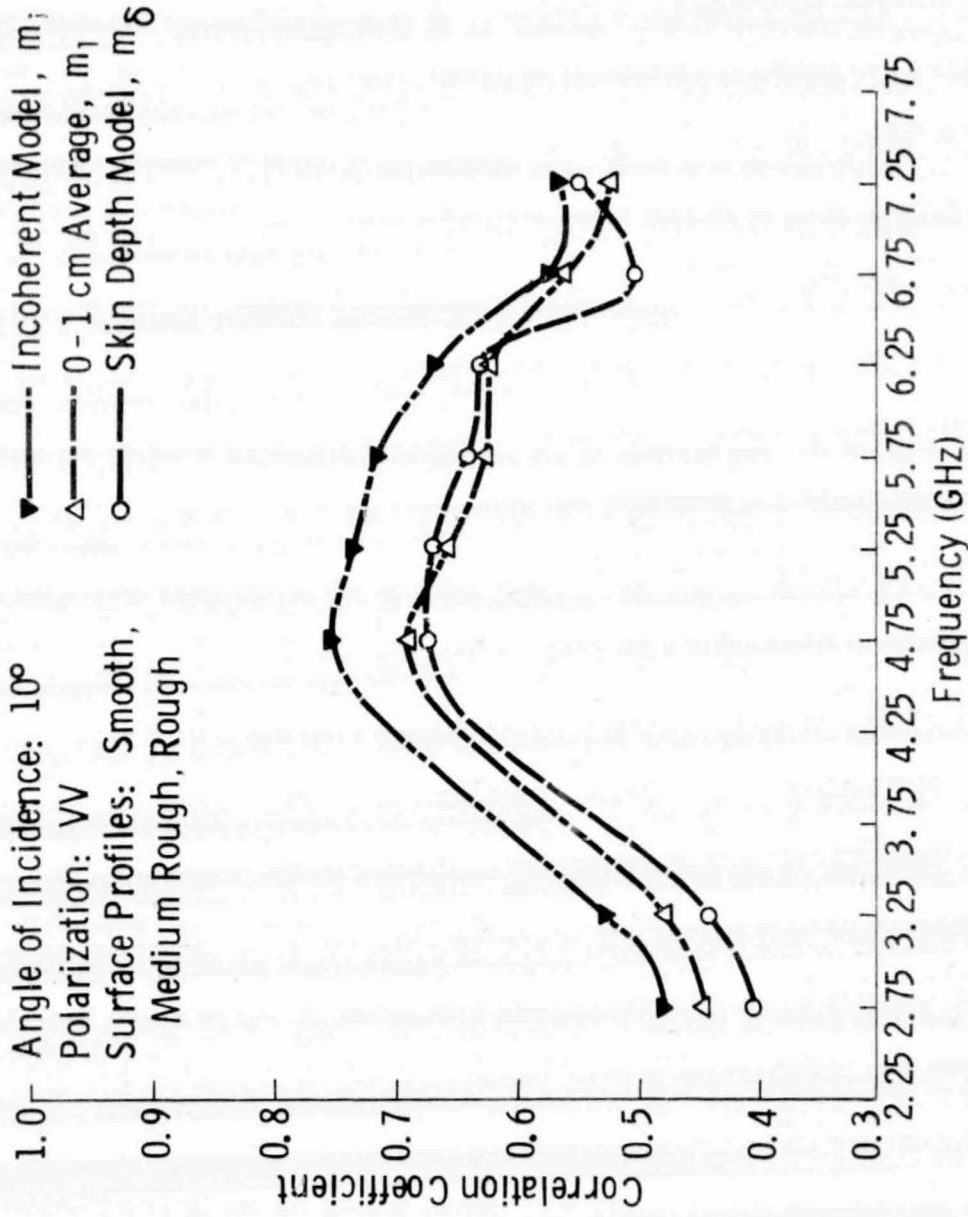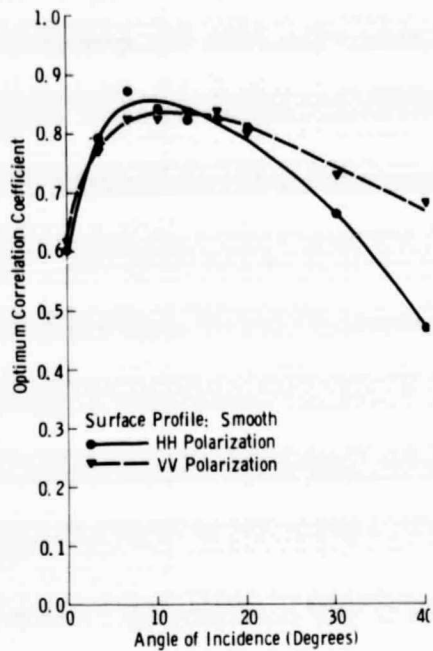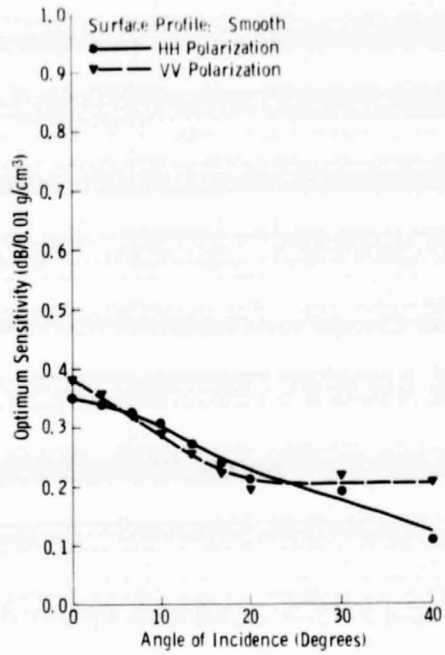
35

Figure 22. Linear correlation coefficient between σ^{-c} and moisture content (with the latter expressed in terms of m_i, m_1, and m_δ) as a function of frequency. Data from all three fields were used in the regression analysis.
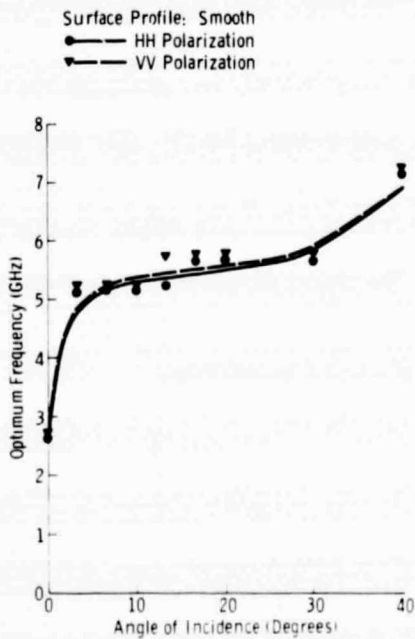
Optimum Correlation Coefficient

1.0
0.9
0.8
0.7
0.6
0.5
0.4
0.3
0.2
0.1
0.0

Surface Profile: Smooth
HH Polarization
VV Polarization

Angle of Incidence (Degrees)
0   10   20   30   40

(a) Optimum Correlation Coefficient

Optimum Sensitivity (dB/0. 01 g/cm³)

1.0
0.9
0.8
0.7
0.6
0.5
0.4
0.3
0.2
0.1
0.0

Surface Profile: Smooth
HH Polarization
VV Polarization

Angle of Incidence (Degrees)
0   10   20   30   40

(b) Optimum Sensitivity

Surface Profile: Smooth
HH Polarization
VV Polarization

Optimum Frequency (GHz)

8
7
6
5
4
3
2
1
0

Angle of Incidence (Degrees)
0   10   20   30   40

(c) Optimum Frequency

Figure 23. Optimum (a) correlation coefficient, (b) sensitivity, and (c) frequency plotted as a function of angle of incidence for the smooth surface profile.

37

An important note should be made regarding these curves. Since the data used to generate the curves covers the band 2.75-7.25 GHz, the true optimum performance at some angles might be at frequencies outside this band. Consider, for example, the end points in Figure 23c. The shape of the curve suggests that at 0° the optimum frequency might have been lower than 2.75 GHz if such data were available. Similarly, at 40°, a frequency higher than 7.25 GHz might give a higher correlation coefficient. In between these angles, however, it is clear that a frequency around 5 GHz is optimum.

Figures 24 and 25 present optimum performance curves for fields M and R respectively. Whereas the optimum frequency increases sharply between 0° and 10° for field S (Figure 23c), the optimum frequency curves for field R (Figure 25c) show a decreasing trend.

## 5.3.2 Moisture Response for Medium and Rough Fields Combined

Optimum performance curves generated on the basis of the combined data from fields M and R are shown in Figure 26. The optimum correlation is a maximum (0.89) at 10° and 2.75 GHz, for both polarizations. In the 0°-20° angular range, the optimum frequency varies within a narrow range between 2.75 GHz and 3.25 GHz.

## 5.3.3 Moisture Response for Smooth, Medium and Rough Fields Combined

When data from all three roughnesses are combined together, the optimum parameters show a strong dependence on angle of incidence. The optimum correlation coefficient (Figure 27a) increases from about 0.66 to 0.75 (for VV polarization) as the angle is varied between nadir and 10°, and then decreases rapidly with angle. The corresponding sensitivity (Figure 27b) decreases approximately exponentially with angle of incidence and the optimum frequency (Figure 27c) increases with angle from 3.25 GHz at nadir to 7.25 GHz for angles higher than 20°. The trend of the optimum frequency curves between nadir and 20° suggests that the optimum frequencies at angles higher than 20° would be higher than 7.25 GHz if such data were available.
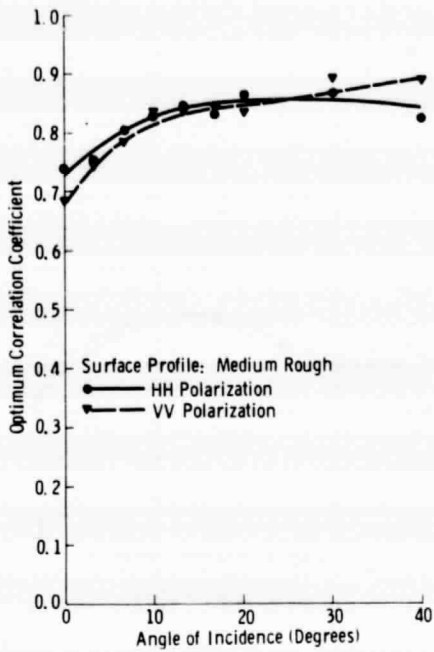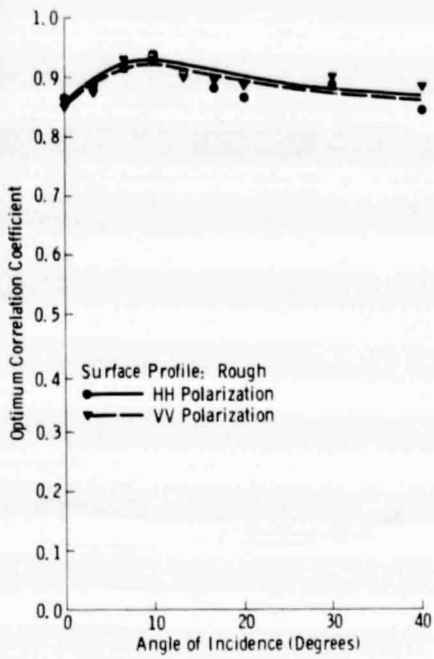
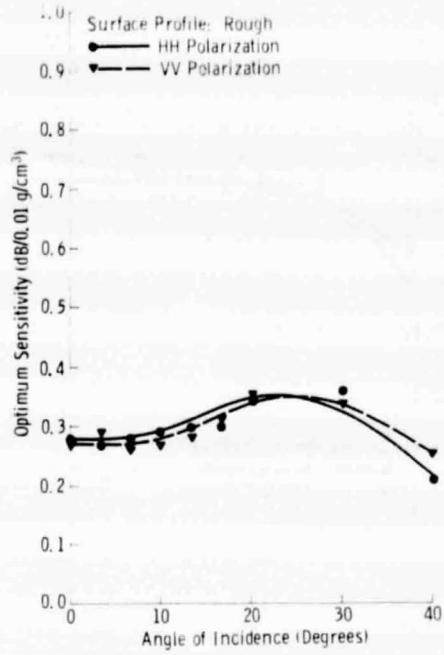(a) Optimum Correlation Coefficient
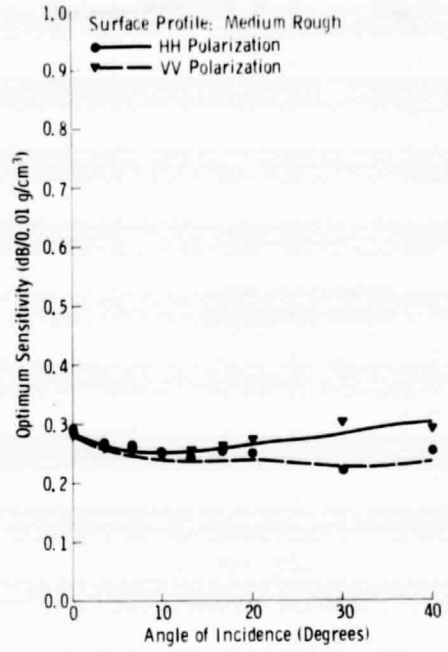
(b) Optimum Sensitivity
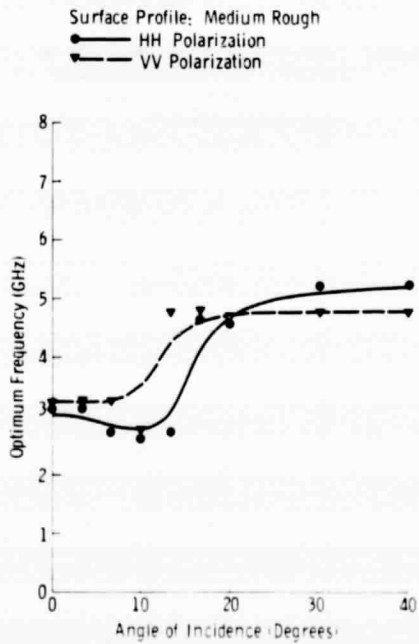
(c) Optimum Frequency

Figure 24. Optimum (a) correlation coefficient, (b) sensitivity, and (c) frequency plotted as a function of angle of incidence for the medium rough surface profile.

39

(a) Optimum Correlation Coefficient

(b) Optimum Sensitivity

(c) Optimum Frequency

Figure 25. Optimum (a) correlation coefficient, (b) sensitivity, and (c) frequency plotted as a function of angle of incidence for the rough surface profile.

40

(a) Optimum Correlation Coefficient
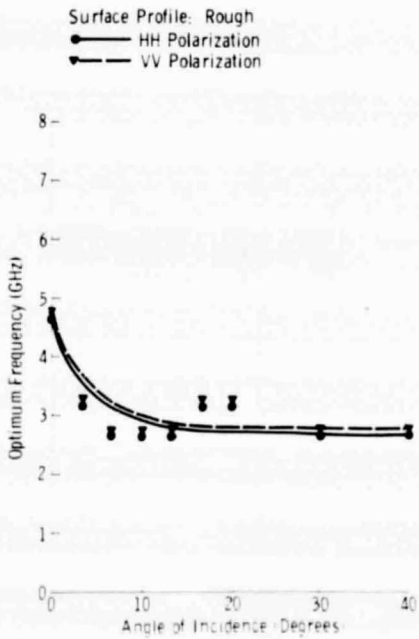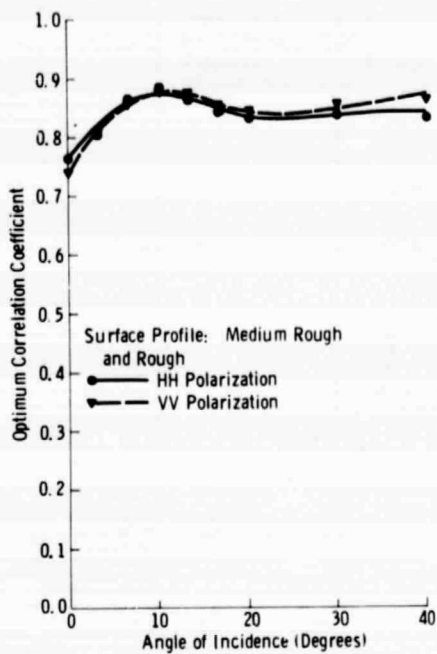

(b) Optimum Sensitivity

(c) Optimum Frequency

Figure 26. Optimum (a) correlation coefficient, (b) sensitivity, and (c) frequency plotted as a function of angle of incidence for the medium rough and rough surface profiles combined.

41

(a) Optimum Correlation Coefficient

(b) Optimum Sensitivity

Surface Profile: Smooth,
  Medium Rough, and Rough
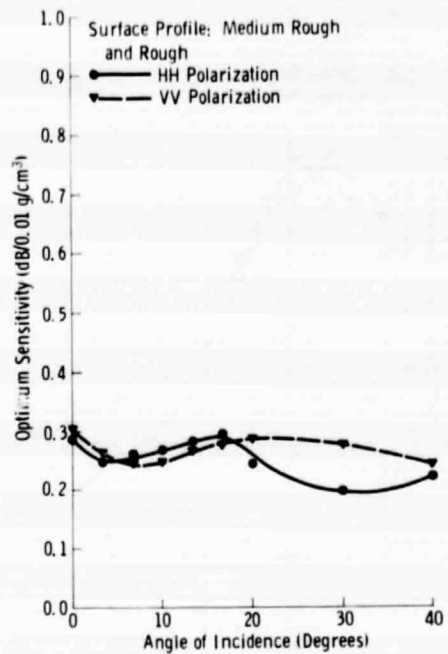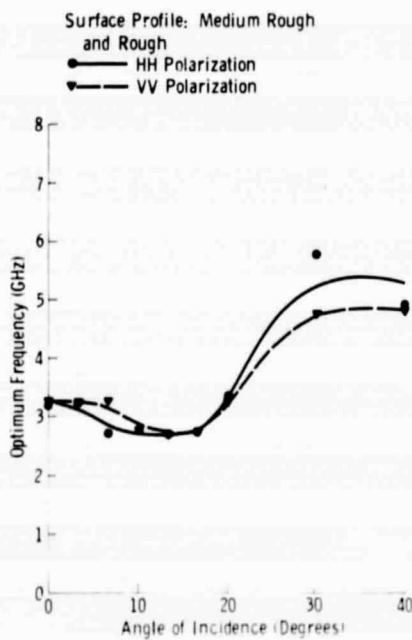 ●——— HH Polarization
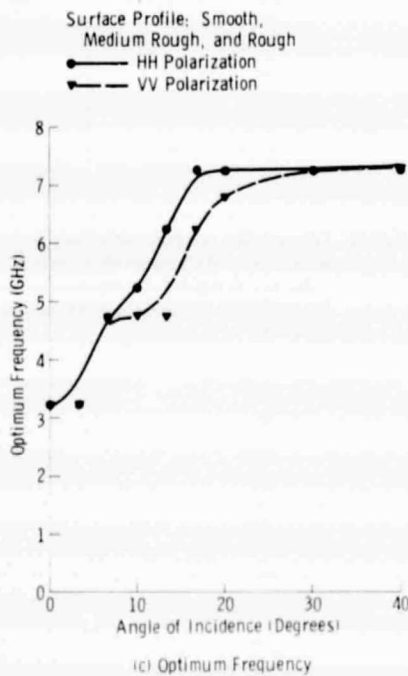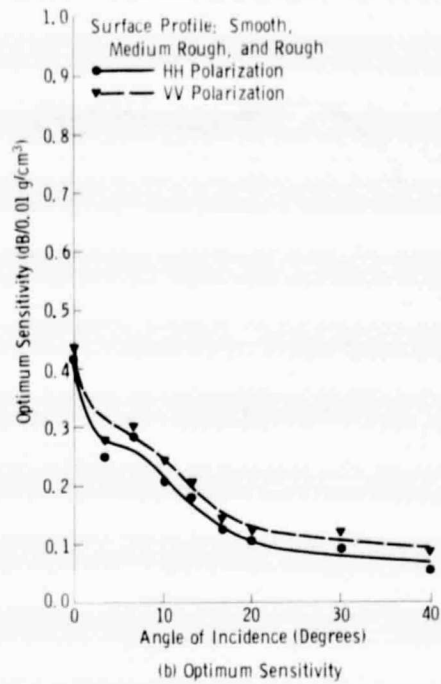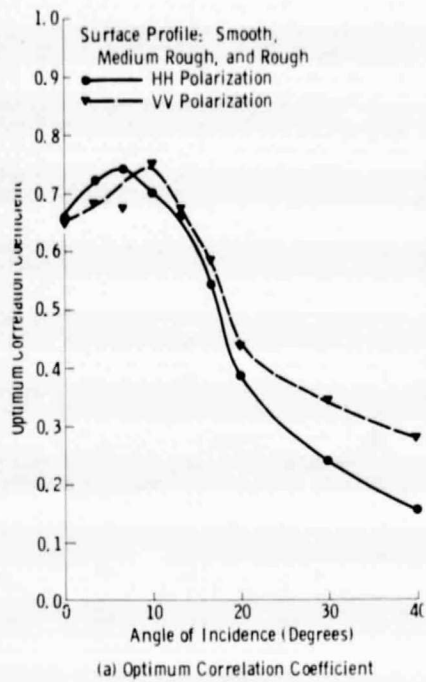 ▼— — VV Polarization

(c) Optimum Frequency

Figure 27. Optimum (a) correlation coefficient, (b) sensitivity, and (c) frequency plotted as a function of angle of incidence for the smooth, medium rough, and rough surface profiles combined.

42

6.0 RECOMMENDATIONS FOR AN OPERATIONAL SYSTEM

As was stated earlier, the surface of field S is a rather rare case in terms of the majority of terrain surfaces. Hence, by including the data of field S to generate the performance curves of Figure 27, we are applying more stringent requirements on the performance of a radar system for detecting soil moisture content than is necessary under most conditions. Excluding field S, on the other hand, means a bias towards rougher surfaces (Figure 26). Hence design parameters for an operational system can be defined as a compromise between those recommended by Figure 26 (Fields M and R only) and those recommended by Figure 27 (all fields).

Based on optimum correlation coefficient and optimum sensitivity considerations, both figures indicate that the angular range extending between about 7° and 15° is optimum. The corresponding optimum frequency, however, is around 3 GHz in Figure 26 and around 5 GHz in Figure 27. As a compromise, 4 GHz is recommended. Over the 7°-15° angular range, HH and VV polarizations appear to have approximately the same soil moisture response.

In summary, the recommended radar parameters are:

Angle of Incidence Range: 7 – 15°

Frequency: 4 GHz

Polarization: HH or VV.

It is most interesting that the above sensor parameters recommended on the basis of radar measurements of bare ground agree perfectly well with 4-8 GHz measurements of vegetated fields reported by Ulaby [5]. Data acquired for a variety of crop types were used to calculate the correlation coefficient between σ^o and soil moisture content. The highest correlation observed was at 10° and 4.7 GHz!

REFERENCES

[1] Hoekstra, P. and A. Delaney, "Dielectric Properties of Soils at UHF and Microwave Frequencies," J. Geophys. Res., vol. 79, no. 11, pp. 1699-1708, 1974.

[2] Cihlar, J. and F. T. Ulaby, "Dielectric Properties of Soils as a Function of Moisture Content," RSL Technical Report 177-47, University of Kansas Center for Research, Inc., Lawrence, Kansas, November, 1974.

[3] Ulaby, F. T., "Radar Measurement of Soil Moisture Content," IEEE Trans. on Antennas and Propagation, vol. AP-22, no. 2, pp. 257-265, March, 1974.

[4] Ulaby, F. T., J. Cihlar and R. K. Moore, "Active Microwave Measurement of Soil Water Content," Remote Sensing of Environment, vol. 3, pp. 185-203, 1974.

[5] Ulaby, F. T., "Radar Response to Vegetation," IEEE Trans. on Antennas and Propagation, vol. AP-23, no. 1, pp. 36-45, January, 1975.

[6] Ulaby, F. T., T. F. Bush and P. P. Batlivala, "Radar Response to Vegetation II: 8-18 GHz Band," IEEE Trans. on Antennas and Propagation, vol. AP-23, no. 5, pp. 608-618, September, 1975.

[7] Oberg, J. M. and F. T. Ulaby, "MAS 2-8 Radar and Digital Control Unit," RSL Technical Report 177-37, University of Kansas Center for Research, Inc., Lawrence, Kansas, October, 1974.

[8] Bush, T. F. and F. T. Ulaby, "Fading Characteristics of Panchromatic Radar Backscatter from Selected Agricultural Targets," IEEE Trans. on Geoscience Electronics, vol. GE-14, October, 1975.

[9] Batlivala, P. P. and J. Cihlar, "Joint Soil Moisture Experiment (Texas): Documentation of Radar Backscatter and Ground Truth Data," RSL Technical Report 264-1, University of Kansas Center for Research, Inc., Lawrence, Kansas, April, 1975.

[10] Poe, G. A., "Remote Sensing of the Near0Surface Moisture Profile of Specular Soils with Multi-Frequency Microwave Radiometry," Proc. SPIE, vol. 27, November, 1971.

[11] Casey, K. F., "Application of Hill's Functions to Problems of Propagation in Stratified Media," IEEE Trans. on Antennas and Propagation, vol. AP-20, no. 3, pp. 368-374, May, 1972.

[12] Moore, R. K., "Ground Echo," Chapter 25 in Radar Handbook by M. I. Skolnik, (Ed)., McGraw-Hill Book Company, New York, 1970.

[13] Burke, W. J. and J. F. Paris, "A Radiative Transfer Model for Microwave Emissions from Bare Agricultural Soils," NASA Document TMX-58166, NASA/JSC, Houston, Texas, August, 1975.